JOURNAL OF QUATERNARY SCIENCE (2018) **33**(8) 905–923 ISSN 0267-8179. DOI: 10.1002/jqs.3068

JQS Journal of Quaternary Science QRA Quaternary Research Association

Holocene relative mean sea-level changes in the Wadden Sea area, northern Netherlands

ERIK W. MEIJLES,[1,2]* PATRICK KIDEN,[3] HARM-JAN STREURMAN,[4] JOHANNES VAN DER PLICHT,[4] PETER C. VOS,[5] W. ROLAND GEHRELS[6] and ROBERT E. KOPP[7,8]

[1]Faculty of Spatial Sciences, University of Groningen, Groningen, The Netherlands
[2]Centre for Landscape Studies, University of Groningen, Groningen, The Netherlands
[3]TNO - Geological Survey of The Netherlands, Utrecht, The Netherlands
[4]Centre for Isotope Research, University of Groningen, Groningen, The Netherlands
[5]Deltares, Utrecht, The Netherlands
[6]Environment Department, University of York, Heslington, York, UK
[7]Department of Earth & Planetary Sciences, Rutgers University, Piscataway, NJ, USA
[8]Institute of Earth, Ocean & Atmospheric Sciences, Rutgers University – New Brunswick, NJ, USA

Received 6 January 2017; Revised 2 July 2018; Accepted 25 July 2018

ABSTRACT: Although the Netherlands has a long tradition of sea-level research, no Holocene relative sea-level curve is available for the north of the country. Previous studies hypothesized that the relative sea-level reconstruction for the western Netherlands is also valid for the northern part of the country. However, glacial isostatic adjustment (GIA) models predict a lower and steeper relative sea-level curve because of greater postglacial isostatic subsidence. Long-term data of relative sea-level change are important to inform GIA models and understand postglacial vertical land motion related to the rebound of Fennoscandia and neotectonic activity. We compiled and evaluated a set of basal peat radiocarbon dates to reconstruct the Holocene relative mean sea-level rise in the Dutch Wadden Sea area. For the early Holocene, this reconstruction is lower than the western Netherlands curve. After 6400 cal a BP, the curve for the Wadden Sea is statistically indistinguishable from that for the western Netherlands, a result that conflicts with GIA model results. It remains to be investigated whether the problem lies with the GIA model predictions or with the quality of the available data. Additional basal peat radiocarbon dates from suitable sites should be collected to further resolve this problem.

KEYWORDS: basal peat; differential land movements; glacial isostatic adjustment; North Sea; radiocarbon dating.

Introduction

Changes in relative sea level (RSL) are caused by a combination of global (glacio-eustatic) sea-level changes and regional land movement. Relative land-level movements in NW Europe are a legacy of its glacial history and the rebound of Fennoscandia. Geological observations of postglacial relative land- and sea-level change in this region constrain models of glacial isostatic adjustment (GIA) (e.g. Lambeck *et al.*, 1998), which in turn are used to understand Earth structure and viscosity parameters of lithosphere and mantle (Vink *et al.*, 2007). GIA models also provide data on vertical coastal land movements for input into future relative sea-level change scenarios (Lowe *et al.*, 2009; Simpson *et al.*, 2017).

Regional Holocene RSL reconstructions provide information on neotectonic activity, palaeogeography and morphological evolution of coastal areas, past tidal ranges, palaeoecology and human settlement history (Beets and Van der Spek, 2000; Kiden *et al.*, 2002; Van de Plassche *et al.*, 2005; Vink *et al.*, 2007; Vött, 2007; Baeteman *et al.*, 2011). In the early Holocene, global sea levels rose rapidly due to the melting of ice caps after the Weichselian glacial period (Fairbanks, 1989; Bard *et al.*, 1996; Smith *et al.*, 2011), with rates in the southern North Sea of more than a metre per century until about 7500 cal a BP (Hijma and Cohen, 2010). The RSL of the southern North Sea continued to rise at a decreasing rate mainly due to isostatic and, to a lesser degree, tectonic subsidence (Kiden *et al.*, 2002; Vink *et al.*, 2007). Since around 3000 cal a BP, the contributions of isostasy and tectonic subsidence to the rise in RSL have been more or less equal for the western Netherlands (Kiden *et al.*, 2008). However, RSL changes in the North Sea area are spatially and temporally variable due to tectonic movements and, in particular, glacio-isostasy (Kiden *et al.*, 2002; Shennan and Horton, 2002; Vink *et al.*, 2007; Shennan *et al.*, 2012). In light of projected sea-level rise due to global warming, there is a need to understand these regional patterns of differential land movements because they are an important contributor to future RSL rise (Gehrels, 2010; Shennan *et al.*, 2012). In the Netherlands, however, vertical land movements have not been considered in some recently published future sea-level projections (Katsman *et al.*, 2011; De Vries *et al.*, 2014; KNMI, 2014). GIA models can make an important contribution to estimates of the land-level component of future RSL projections in the Netherlands, as they have done in the UK (Lowe *et al.*, 2009) and around the world (Kopp *et al.*, 2014).

Holocene RSL curves have been constructed with great precision for most coastal areas in the Netherlands and adjacent regions (Figs 1 and 2). The reconstructions are indicative for the local mean sea level and therefore they are referred to as 'relative mean sea-level' (relative MSL; Kiden *et al.*, 2002; Berendsen *et al.*, 2007; Hijma and Cohen, 2010). For the western Netherlands, a long history of relative MSL reconstruction includes the curves by Jelgersma (1961) and Van de Plassche (1981, 1982), with recent adjustments and extensions in time provided by Berendsen *et al.* (2007),

*Correspondence: Erik W. Meijles, as above.
E-mail: e.w.meijles@rug.nl

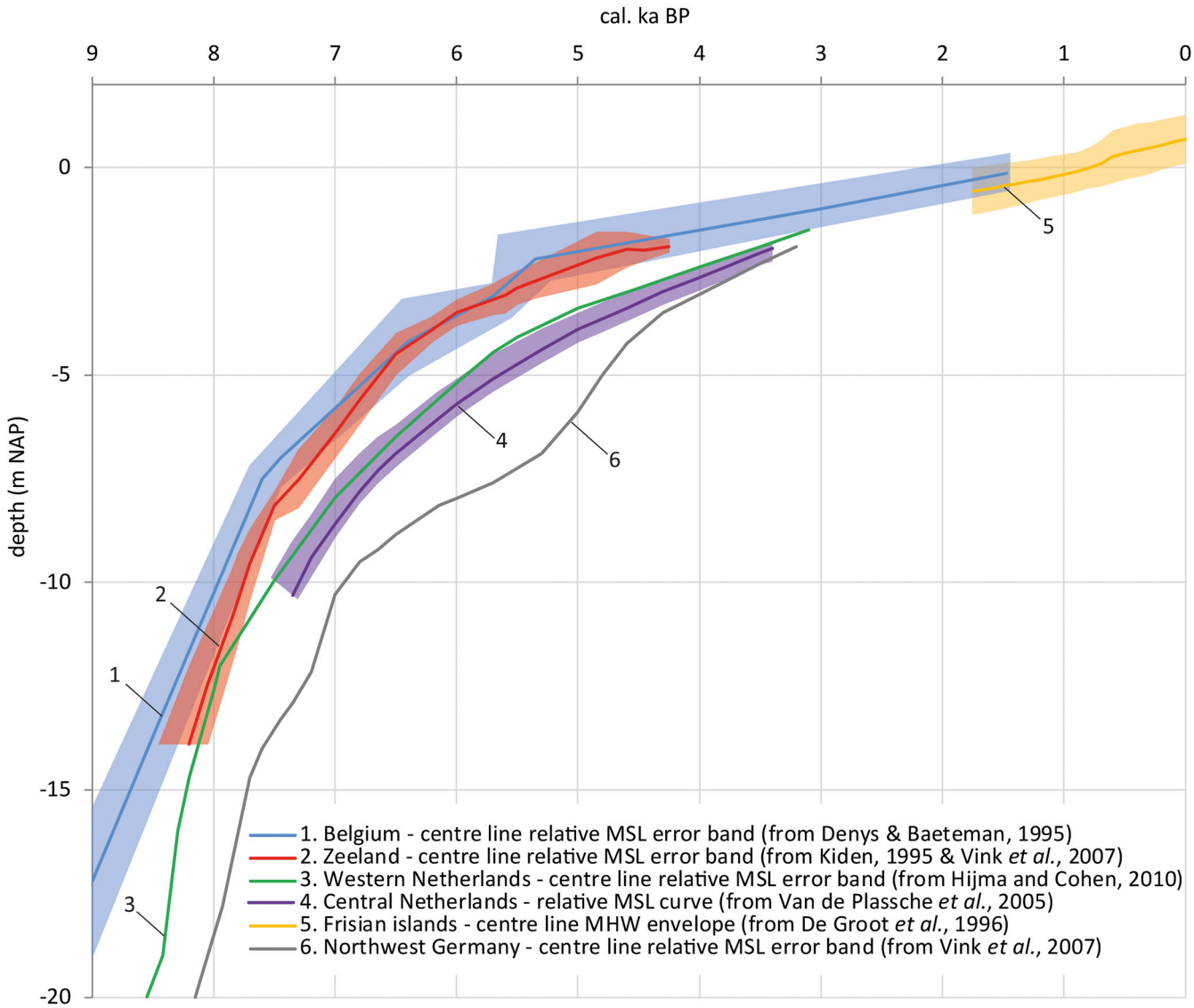

Figure 1. Holocene relative MSL curves with their error bands (if available) for the Netherlands and adjacent regions.

Hijma and Cohen (2010) and Van de Plassche *et al.* (2010) among others. Further inland, Van de Plassche *et al.* (2005) provided a relative MSL curve for the Flevo area of the central Netherlands. For the south-western Netherlands and Belgium, relative MSL reconstructions were made by Kiden (1995) and Denys and Baeteman (1995). For the German Wadden Sea region, several curves are available (e.g. Ludwig *et al.*, 1981; Streif, 1989, 2004). The most recent curve for this region was created by Behre (2007), although its interpretation is highly debated (e.g. Bungenstock and Weerts, 2010, 2012; Baeteman *et al.*, 2011, 2012; Behre, 2012a,b).

Despite the research in past decades on the coastal development of the northern Netherlands (e.g. Jelgersma, 1961; Roeleveld, 1974; Griede, 1978), no sea-level curve exists for the Dutch Wadden Sea covering the Holocene period. Van de Plassche (1982) suggested, on the basis of only two reliable sea-level index points (SLIPs) from Jelgersma (1961), that the relative MSL curve of the Wadden Sea region is similar to the western Netherlands curve. However, based on GIA models of Lambeck *et al.* (1998), Kiden *et al.* (2002) suggested that, as the Wadden Sea area is situated closer to the last glacial Scandinavian ice sheet, the collapse of the forebulge drives larger subsidence in this area than in regions further south. The influence of the British ice sheet is minimal here due to its relatively small volume (Kiden *et al.*, 2002). Kiden *et al.* (2002) and Vink *et al.* (2007) inferred that the central part of the peripheral bulge, subject to the greatest degree of Holocene isostatic subsidence, is probably located under the German Bight and the Dutch sector of the North Sea, a pattern that is also predicted by the GIA model of Lambeck *et al.* (1998). This suggest that post-glacial subsidence rates are higher in the northern Netherlands, resulting in a lower and steeper relative MSL curve than in the western Netherlands.

Although the Dutch Wadden Sea is part of a UNESCO World Heritage Site, it is currently affected by human-induced subsidence due to natural gas extraction, which increases subsidence above its background, natural rate. New RSL data help to constrain the history of the forebulge collapse during the Late Pleistocene/Holocene and is also useful for determining the role of the associated RSL rise in the development of the Wadden Sea area and the bordering mainland (Speelman *et al.*, 2009). Holocene RSL data in combination with GIA model simulations and palaeogeographical reconstructions can inform and optimize future management of the Wadden Sea.

The objective of this paper is three-fold. Firstly, we aim to increase the number of sea-level index points for the Dutch

Figure 2. Study area in relation to regionally adjacent relative MSL reconstructions.

Wadden Sea region based on a new compilation and evaluation of archived published and unpublished radiocarbon age determinations of coastal basal peat samples. Secondly, using this data set, we reconstruct a Holocene relative MSL curve for the Dutch Wadden Sea region and discuss the reliability of the data for this purpose. Thirdly, we compare the relative MSL curve with curves from adjacent regions in the southern North Sea to test the hypothesis that the curve is comparable to the western Netherlands curve, implying negligible differential land movements between the two areas.

Methodology

Use of basal peat for relative MSL reconstructions

In the coastal zone of the Netherlands basal peat deposits present at the base of the Holocene have been used in a substantial number of early Holocene sea-level reconstructions (e.g. Bennema, 1954; Jelgersma, 1961). Holocene relative MSL reconstructions in the Netherlands and many other coastal lowlands in the North Sea region have been traditionally based on ^{14}C dating of samples from the base of peat beds (the so-called 'basal peat') lying directly on top of the sandy Pleistocene subsurface (Bennema, 1954; Van Straaten, 1954; Jelgersma, 1961; Van de Plassche, 1982; Denys and Baeteman, 1995; Kiden, 1995; Streif, 2004; Shennan *et al.*, 2006; Vos, 2015). These basal peat dates are particularly suitable to assess relative MSL rise, as the compaction of the underlying Pleistocene deposits can be considered negligible on the time-scale of the Holocene.

Basal peat formation

Basal peats were formed during the late Pleistocene and Holocene when local groundwater levels rose in response to the rising sea level that gradually submerged the sloping Pleistocene surface. Upwards groundwater seepage due to the reduced natural drainage of the area made the Pleistocene surface increasingly wet and created favourable conditions for peat formation. The basal peat therefore developed indirectly under the influence of RSL rise. As the sea level rose, the zone of basal peat growth gradually moved landwards and into higher areas, while the lower-lying peat was covered by coastal deposits (Kiden *et al.*, 2008; Vos, 2015). In this way, a relatively thin but extensive layer of basal peat developed on top of the sloping Pleistocene surface.

The formation of basal peat was much reduced, if not halted, when the sea-level rise slowed down during the Holocene, and freshwater fenlands were replaced by salt marshes and tidal flats (Streif, 2004). In some areas, the peat was eroded by wave action and tidal channel erosion, but in other places the peats were covered by marine deposits (Vos, 2015).

Indicative meaning of data points

One of the basic assumptions underpinning relative MSL studies is that, in the temperate humid climate of the Netherlands in the Holocene, freshwater peat growth in the coastal plain takes place at or above, but never lower than MSL at that location (Bennema, 1954; Jelgersma, 1961;

Van de Plassche, 1982; Roep and Beets, 1988; Van de Plassche and Roep, 1989; Kiden, 1995; Kiden *et al.*, 2002; Hijma and Cohen, 2010). It is generally accepted that basal peat starts forming at local MSL or, when there is tidal influence, at mean high water level (MHW) (Van de Plassche, 1982; Kiden *et al.*, 2002, 2008).

The altitude of basal peat growth relative to MSL is also a function of the local mean tidal range and river influences (Van de Plassche, 1980, 1982; Vink *et al.*, 2007; Baeteman *et al.*, 2011). In a tidal basin, tidal amplitude may be attenuated due to the accommodation of the flood volume in the intertidal area of the basin and due to frictional loss of mechanical energy. This flood basin effect reduces the local MHW level relative to coastal MHW (Van de Plassche, 1982). In contrast, MHW level may be raised in a landward direction away from the coast due to tidal amplification in tidal basins or estuaries and due to river and groundwater table gradients (Van de Plassche, 1982; Kiden, 1995; Baeteman *et al.*, 2011). In a tidally influenced area, the position of the basal peat can therefore strictly speaking only be used to reconstruct the upper limiting relative MSL curve (Vink *et al.*, 2007). In local depressions, at sites with impermeable soil layers and in (nearly) flat areas further away from direct marine influence, peat formation can also be driven by local groundwater conditions, completely independent of sea-level rise (Van de Plassche, 1981; Kiden, 1995; Shennan and Horton, 2002). In these situations, the sea-level index points are 'limiting', meaning that they were formed above MSL, by an unknown vertical distance, but they can never be lower than local MSL.

In areas close to the sea where the Pleistocene surface is steep, the zone of coastal peat formation is relatively narrow and basal peat growth is mainly controlled by the sea level. As a consequence, dated freshwater basal peat samples are groundwater-level index points that can be used to define an upper limit for relative MSL rise (Van de Plassche and Roep, 1989; Shennan and Horton, 2002; Hijma *et al.*, 2015). In other words, actual relative MSL should be at or below the lowest basal peat index points but, when carefully selected from a sloping substrate, and when a large number of such data points are available, such as in the western Netherlands (Hijma and Cohen, 2010) or the Mississippi Delta (Törnqvist *et al.*, 2004), it is possible to define a true relative MSL curve from the lowest basal peat data (Van de Plassche, 1982; Hijma and Cohen, 2010).

When using basal peats for relative MSL reconstructions it is therefore important to distinguish between sites where peat was formed as a response to local groundwater conditions and sites where a rising sea level was the trigger (Van de Plassche, 1982; Cohen, 2005). Detailed information on the Pleistocene subsurface topography is essential. In addition, in some coastal peats, macro remains evident of marine influence can be used as SLIPs, but these indicators are rare in basal peats in the Netherlands. Careful screening of the individual data points is therefore needed to obtain insight into the difference in groundwater or relative MSL rise from site to site. We use the term 'index point' here for samples from sites that we infer to be controlled by sea-level rise.

Peat sample treatment and radiocarbon dating

To collect new sea-level data for this study, we searched the archives of the Groningen Centre for Isotope Research (CIO) for previously unpublished peat age determinations. Most of the peat samples were by-products of mapping surveys and were not collected for sea-level reconstructions. All peat samples were dated and archived at the CIO between around 1958 and 2013. Samples underwent pre-treatment, consisting of a physical and a chemical component. Sand, clay and roots that penetrated the peat were removed. A standard acid–alkali–acid (AAA) pre-treatment with HCl, NaOH and again HCl (Mook and Streurman, 1983; Mook and Van de Plassche, 1986) was used to isolate the stable chemical fraction for dating, and remove contaminants, including allochthonous fossil organic matter, organic (humic) infiltration and secondary carbonate.

After pre-treatment the samples were combusted to CO_2. Most samples shown in Table 1 were measured by the conventional method (laboratory code GrN), requiring relatively large (bulk peat) samples. The ^{14}C radioactivity was measured in the CO_2 gas by proportional gas counting (e.g. Cook and Van der Plicht, 2013). More recently, smaller samples were measured by accelerator mass spectrometry (AMS) (Van der Plicht *et al.*, 2000; laboratory code GrA in Table 1).

For both methods the measured ^{14}C contents are translated into ^{14}C ages. These are conventional dates, reported in BP (Before Present; Present = ad 1950), based on the original half-life value of 5568 years and includes correction for isotopic fractionation using the stable isotope ^{13}C to $\delta^{13}C = -25‰$ (Mook and Streurman, 1983). We note that stable isotope measurements and the fractionation correction were introduced around 1960 (Kiden, 1995; Mook, 2005). Samples dated before 1960 were not corrected and $\delta^{13}C$ values for these samples are not available. Since peat has $\delta^{13}C$ values of -27 to -28 ‰ and each per mil change in $\delta^{13}C$ corresponds to a correction of 16 ^{14}C years (Mook, 2005), these samples were corrected by making the ^{14}C age 45 years younger. This is the case for the samples in Table 1 with numbers GrN-2424 and lower. These were originally GrO dates; to avoid confusion, they were reassigned as GrN dates after applying the mentioned estimated fractionation correction (for details see Vogel and Waterbolk, 1963). We also note that the fractionation correction for peat is small compared with the typical measurement uncertainties for these dates (quoted in Table 1 as 1σ uncertainties).

The conventional ^{14}C dates were calibrated into calendar years using the calibration curve IntCal13 (Reimer *et al.*, 2013) and the computer program Oxcal (Bronk Ramsey, 1995, 2001). The calibrated age range and medians are shown in Table 1 in cal a BP.

Index point selection

To identify peat samples within a database that can be used as index points, we used two criteria: the authors' original interpretation of the samples and the position on the time–depth diagram. By drawing a line through the upper error limits of the lowest samples in the time–depth diagram, the samples in the zone above this line can be identified as too old or too high to be deemed index points. They have probably formed in a landscape position that is independent of sea level and therefore we interpreted them as 'controlled by local groundwater conditions' (Supporting Information S1). The samples that do not reflect the relative MSL at their locations are outlined in the section 'Indicative meaning of data points'. We interpreted the samples below the line as having the 'lowest local time–depth position' and thus forming potential index points. These lowest samples with their respective error margins provide an upper limit for relative MSL (Denys and Baeteman, 1995). As we adopt the same methodology as relative MSL reconstructions for Belgium, Zeeland and the Western and Central Netherlands, it is possible to compare the relative position of MSL curves.

Table 1. All radio carbon age determinations used for this study.

No.	Lab. code	*X* (RD)*	*Y* (RD)*	Sample depth (m)†		Uncertainty (m)		Material	Position‡	^{14}C age (BP)	Calibr. age range (cal a BP, 2σ)	References
				From	To	Lower	Upper					
1	GRN-30128	244250	583000	−4.43	−4.47	0.22	0.22	Gyttja	bbp	10 290 ± 250	12 665–11 280	Woldring *et al.* (2005)/CIO§
2	GRN-7565	198100	599100	−9.87	−9.91	0.22	0.22	Peat, unclassified	bbp	9290 ± 55	10 650–10 280	Griede (1978)
3	GRN-17869	259100	579100	?	?	0.54	0.54	Peat, unclassified	bbp	8420 ± 85	9550–9140	RGD/CIO§
4	GRN-32801	239500	582800	?	?	0.54	0.54	Peat, unclassified	bbp	8210 ± 70	9405–9010	CIO§
5	GRA-2424	115136	584899	−17.09	−17.10	1.02	1.02	Peat with sand	bbp	7490 ± 70	8410–8175	RGD/CIO§
6	GRA-2423	115136	584899	−17.09	−17.10	1.02	1.02	Peat with sand	bbp	7340 ± 70	8330–8010	RGD/CIO§
7	GRN-23923	247910	599140	−10.30	−10.35	0.23	0.23	Peat, unclassified	bbp	7320 ± 60	8310–8005	Kiden and Vos (2012)
8	GRN-23931	243300	607300	−16.06	−16.10	0.22	0.22	Peat, unclassified	bbp	7170 ± 25	8020–7945	RGD/CIO§
9	GRN-18285	177205	604425	−13.53	−13.56	1.02	1.02	Wood peat	bbp	7095 ± 50	8015–7830	Van der Spek (1994)
10	GRN-18286	177205	604425	−13.56	−13.62	1.02	1.02	Mor, sandy	bbp	7025 ± 50	7960–7740	Van der Spek (1994)
11	GRN-23922	245180	607330	−14.23	−14.26	0.22	0.22	Peat, unclassified	bbp	6980 ± 40	7930–7700	Kiden and Vos (2012)
12	GRN-7568	181500	591200	−6.36	−6.40	0.22	0.22	Peat, unclassified	bbp	6930 ± 45	7920–7670	Griede (1978)
13	GRN-21613	229700	590900	−12.17	−12.20	0.22	0.22	Wood peat	bbp	6930 ± 30	7835–7685	Kiden and Vos (2012)
14	GRN-21610	227080	590700	−10.32	−10.36	0.22	0.22	Wood peat	bbp	6730 ± 50	7675–7505	Kiden and Vos (2012)
15	GRN-621	258500	593500	−6.17	−6.20	0.22	0.22	Fen wood peat	bbp	6420 ± 145	7580–7000	Jelgersma (1961)
16	GRN-606	193500	599500	−6.62	−6.65	0.22	0.22	*Eriophorum* peat	bbp	6255 ± 140	7435–6795	Jelgersma (1961)
17	GRN-23928	251830	594450	−8.42	−8.47	0.23	0.23	Clayey peat	bbp	6220 ± 30	7250–7010	RGD/CIO§
18	GRN-8398	197000	593100	−2.69	−2.70	0.73	0.73	Peat, unclassified	bbp	6060 ± 60	7160–6750	RGD/CIO§
19	GRA-58275	221832	585631	−1.78	−1.79	0.22	0.22	Peat, unclassified	bbp	6050 ± 40	7005–6785	CIO§
20	GRN-7562	186500	589300	−3.40	−3.45	0.23	0.23	Peat, unclassified	bbp	5890 ± 40	6835–6630	Griede (1978)
21	GRN-7641	206500	593500	−7.01	−7.05	0.22	0.22	Peat, unclassified	bbp	5800 ± 40	6720–6490	Griede (1978)
22	GRN-32146	240000	583250	−2.63	−2.65	0.54	0.54	Peat, unclassified	bbp	5320 ± 50	6275–5945	CIO‡
23	GRN-17934	239600	588200	−5.05	−5.10	0.54	0.54	Peat, unclassified	bbp	5250 ± 60	6190–5910	Woldring *et al.* (2005)/CIO‡
24	GRN-637	258500	593500	?	?	0.23	0.23	Clayey fen peat	bbp	5210 ± 150	6290–5655	Jelgersma (1961)¶
25	GRN-06738	237700	584700	−3.75	−3.95	0.55	0.55	Peat, unclassified	bbp	5060 ± 60	5920–5660	CIO‡
26	GRN-1091	269000	578000	−4.19	−4.23	0.22	0.22	Fen peat	bbp	5010 ± 80	5910–5600	Jelgersma (1961)§
27	GRN-26214	231000	592000	−3.84	−3.90	0.23	0.23	Peat, unclassified	bbp	4980 ± 70	5895–5600	CIO§
28	GRN-18021	245000	583750	−2.30	−2.35	0.54	0.54	Peat, unclassified	bbp	4940 ± 100	5915–5470	Woldring *et al.* (2005)/CIO‡
29	GRN-17980	229725	581700	?	?	0.54	0.54	Sandy peat	bbp	4840 ± 100	5880–5320	CIO§
30	GRN-7644	180500	585500	−4.26	−4.31	0.23	0.23	Peat, unclassified	bbp	4760 ± 30	5590–5330	Griede (1978)
31	GRN-24506	188425	591250	−3.64	−3.67	0.22	0.22	Amorph. peat with sand	bbp	4610 ± 120	5595–4960	CIO§
32	GRN-1088	269000	578000	−2.98	−3.03	0.23	0.23	Fen peat	bbp	4310 ± 75	5275–4625	Jelgersma (1961)¶
33	GRN-17981	230300	581700	?	?	0.54	0.54	Peat, unclassified	bbp	4100 ± 80	4830–4430	CIO§
34	GRN-11969	260800	591800	?	?	0.35	0.35	Sandy peat	bbp	3805 ± 35	4385–4085	Bakker (1992)
35	GRN-1090	269000	578000	−1.87	−1.92	0.23	0.23	Fen peat	bbp	3310 ± 60	3690–3400	Jelgersma (1961)¶
36	GRN-1089	269000	578000	−0.90	−0.94	0.22	0.22	Fen peat	bbp	2910 ± 70	3320–2860	Jelgersma (1961)¶
37	GRN-6989	126550	587275	−1.16	−1.17	0.22	0.22	Sandy peat	bp	2785 ± 55	3035–2760	De Jong (1984)
38	GRN-17891	255300	581150	?	?	0.54	0.54	Sandy peat	bbp	2740 ± 70	3005–2740	CIO§
39	GRN-10248	128500	588750	−0.96	−0.97	0.54	0.54	Peat, slightly sandy**	bp	2370 ± 70	2715–2180	De Jong (1984)
40	GRN-7258	146410	600660	−0.07	−0.15	0.54	0.54	*Phragmites* peat	bp	1620 ± 50	1690–1390	De Jong (1984)
41	GRN-7260	146010	600860	0.90	0.86	0.54	0.54	Sandy peat	bp	1555 ± 50	1550–1345	De Jong (1984)
42	GRN-17208	133690	591240	0.20	0.16	0.22	0.22	Peat, slightly sandy	ts	1530 ± 30	1525–1350	De Groot *et al.* (1996)

continued

Table 1. (*Continued*)

No.	Lab. code	*X* (RD)*	*Y* (RD)*	Sample depth (m)†		Uncertainty (m)		Material	Position‡	^{14}C age (BP)	Calibr. age range (cal a BP, 2σ)	References
				From	To	Lower	Upper					
43	GRN-9424	133700	591325	−0.04	−0.08	0.54	0.54	Sandy peat	ts	1500 ± 30	1520–1310	De Jong (1984)
44	GRN-17592	153260	601830	0.23	0.18	0.23	0.23	Clay, humic (residue)	tc	1285 ± 30	1285–1175	De Groot *et al.* (1996)
45	GRN-17597	144750	597820	0.54	0.51	0.22	0.22	Gyttja, slightly sandy	ts	1260 ± 50	1290–1070	De Groot *et al.* (1996)
46	GRN-17594	153300	601700	0.55	0.52	0.28	0.35	Peat, slightly clayey	ts	880 ± 45	915–700	De Groot *et al.* (1996)
47	GRN-7265	146630	598760	−0.09	−0.15	0.54	0.58	Peat, unclassified	ts	655 ± 45	680–550	De Jong (1984)
48	GRN-16935	204885	610365	1.08	1.01	0.23	0.23	Peat, slightly sandy**	ts	525 ± 30	630–505	De Groot *et al.* (1996)
49	GRN-17004	205770	611295	1.67	1.58	0.23	0.23	Sand, humic	ts	455 ± 90	645–305	De Groot *et al.* (1996)
50	GRN-16022	184900	606950	1.25	1.23	0.22	0.22	Clay, strongly peaty††	ts	375 ± 25	505–315	De Groot *et al.* (1996)
51	GRN-17212	130660	588275	1.10	1.08	0.22	0.22	Peat/gyttja, sandy	ts	270 ± 35	460–150	De Groot *et al.* (1996)

*Rijksdriehoekstelsel (Dutch coordinate system).
†Relative to NAP (Dutch Ordnance Datum, approximately present mean sea level).
‡Stratigraphic position: bbp = base basal peat; bp = base of peat; ts = top sand; tc = top clay.
§RGD/CIO: archives of the Dutch Geological Survey/Centre for Isotope Research, respectively (previously unpublished).
¶δ^{13}C error corrections (45 bp; pre-1962).
**With *Phragmites* remains.
††Slightly sandy.

Even if there is bias in the approach, it should be systematic across the sites being compared.

Data collection and evaluation

Study area

The study area comprises the Dutch Wadden Sea region, including bordering mainland and the southern fringe of the North Sea. It is part of a larger, mostly undisturbed intertidal ecosystem stretching from the Netherlands in the west via Germany into Denmark to the north-east. It comprises barrier islands, tidal basins and (diked) salt marshes and, except for the river Ems, has limited river influences (UNESCO, 2009; Bazelmans *et al.*, 2012). It is bordered on the mainland by reclaimed coastal wetlands. During Holocene sea-level rise, coastal wetlands developed in the Pleistocene valley systems due to an increase in (local) groundwater levels. Later, many of the fens were covered by salt marsh sediments or were eroded due to marine ingressions. Since the 11th century, most of the salt marshes have been diked (Vos, 2006, 2015).

The area measures roughly 150 km by 35 km and is comparable in size to adjacent regions for which Holocene relative MSL reconstructions have been established (Figs 2 and 3).

Data sets

Our literature and archival searches yielded a dataset of 51 radiocarbon age determinations of the base of the basal peat. All samples are from the mainland of the two northern provinces of the Netherlands (Fryslân and Groningen) as well as from offshore locations (Fig. 4). Sampling sites further north in the North Sea (e.g. White Bank; Ludwig *et al.*, 1981 and Dogger Bank; Shennan *et al.*, 2000) were not used in the MSL reconstruction, as we consider them to have a different isostatic and tectonic subsidence history than the Wadden Sea region (Kiden *et al.*, 2002; Vink *et al.*, 2007). Sampling sites further inland were also excluded because peat development here was assumed to be a function of the local water table and decoupled from sea level (e.g. Kiden, 1995).

All samples used were basal peat samples, taken at the direct contact with the underlying Pleistocene substrate, and therefore immune to compaction problems. The data are listed in Table 1 and arranged in descending ^{14}C age. The data comprise different (un)published sources, which are described in more detail below. The full dataset, including details on the error calculations, is presented in the Supporting Information (S1).

Jelgersma (1961)

For a study on Holocene relative MSL changes, Jelgersma (1961) collected peat samples in the coastal area of the northern Netherlands from mechanically drilled boreholes and deep excavations. The locations were restricted to sites where the Pleistocene subsurface sloped towards the sea. Samples were selected on the basis of peat type: oligotrophic *Sphagnum* species, indicative of precipitation and independent of phreatic groundwater were discarded. The original data as published by Jelgersma (1961) were not corrected for the Suess and isotopic fractionation effects (^{13}C correction). In a later paper, Jelgersma (1966) corrected for the Suess effect in a time–depth diagram. In Table 1, we show the corrected data (based on the ^{13}C corrected data as presented by Van de Plassche, 1982). Error treatment is described in the next section.

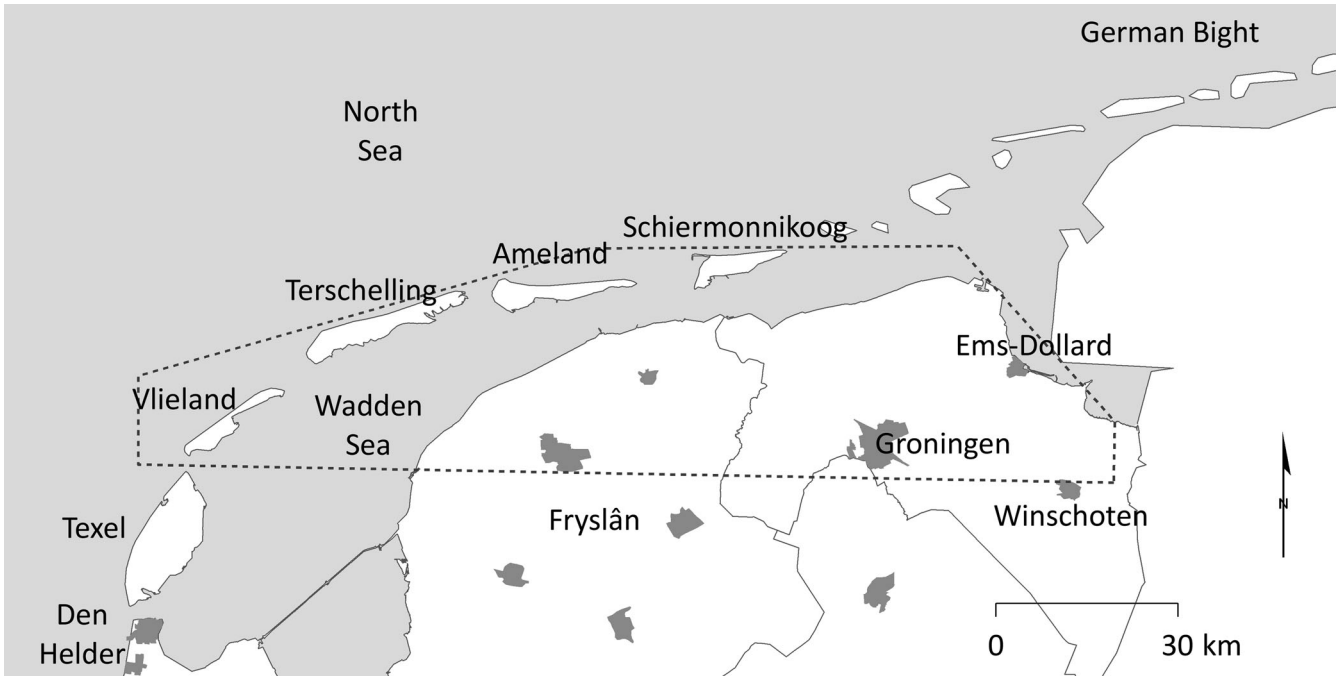

Figure 3. Location map of the study area.

Griede (1978)

Griede (1978) collected basal peat data to study the Holocene coastal evolution of the province of Fryslân. Undisturbed peat samples were retrieved by hand corings. Griede used 17 peat samples in total for radiocarbon dating, of which five were from the base of the basal peat. These data were used in this paper (Table 1). As Griede (1978) is unclear about the levelling methods used, a larger vertical error margin was applied to the data.

De Jong (1984)

As part of surveys for the geological mapping of the Frisian Islands, De Jong (1984) published results of mechanical drillings in coastal dunes. De Jong (1984) and Van Staalduinen (1977) presented samples from peat resting on Holocene sandy marine or wind-blown dune deposits from the Frisian Islands in the Dutch Wadden Sea. Although these samples are strictly speaking not to be regarded as basal peat, they rest on nearly compaction-free sediments. Information on the coring method was limited, although it was noted that some samples were taken with hand-operated Van der Staay suction-corers (Van de Meene *et al.*, 1979) while in other cases continuous cores were recovered using mechanical drilling equipment. As the method of levelling is not documented, we adopted a relatively large vertical error on all samples from De Jong (1984).

Van der Spek (1994, 1996)

Two samples for radiocarbon dating were taken by Van der Spek (1996) from the same continuously cored borehole

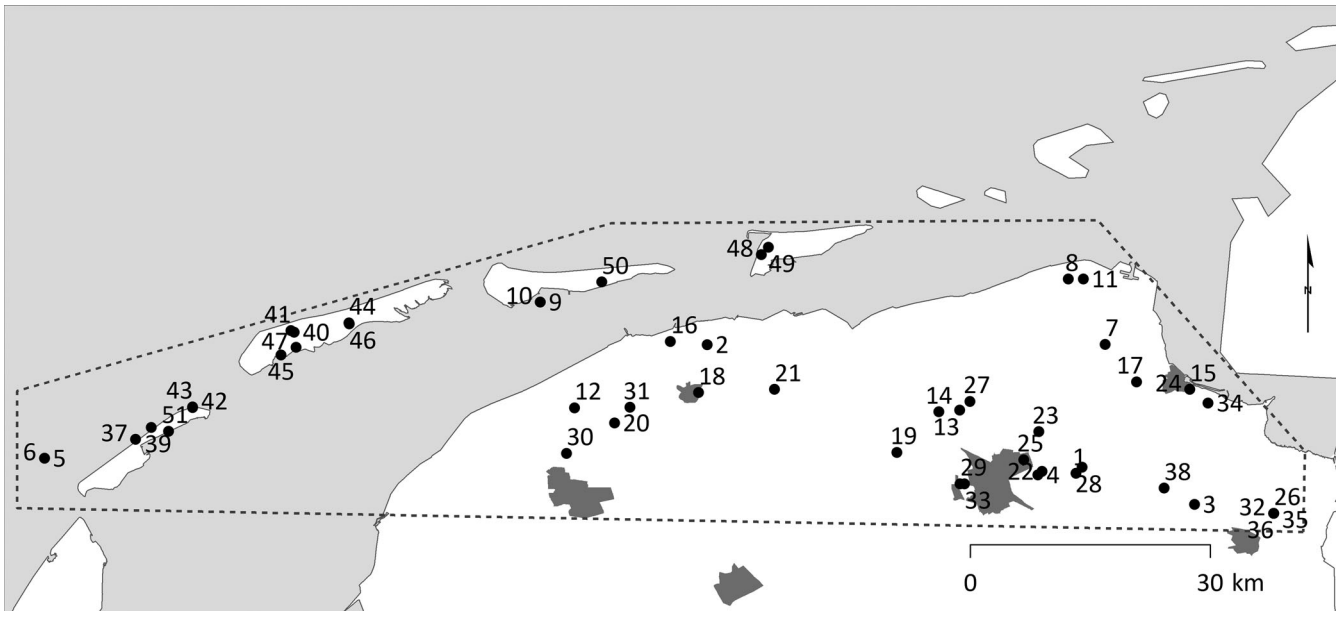

Figure 4. Basal peat sampling sites for the Wadden Sea region. Numbers refer to Table 1.

directly south of the Frisian island of Ameland. The peat was situated under Holocene intertidal deposits. The upper sample is from wood from the base of a compacted basal peat layer; the lower sample is a sandy soil with root traces developed in the uneroded Pleistocene subsurface.

De Groot et al. (1996)

De Groot *et al.* (1996) collected sedimentological data, peat and humic sand samples to document RSL rise in the Frisian Islands over the last 2500 years. The samples rested on (nearly) compaction-free Holocene sandy marine or wind-blown dune deposits and were formed around the MHW level. All but one of the samples were taken from mechanically drilled boreholes, and one sample was taken from an excavation. All sites were levelled to local NAP (Dutch Ordnance Datum; approximately present MSL) benchmarks.

Woldring et al. (2005)

Woldring *et al.* (2005) used basal peat samples to establish the early Holocene landscape evolution of the province of Groningen. The levelling method of the sites is not well documented in the paper. We retrieved surface level altitudes from high-resolution LIDAR data (AHN2; Van der Zon, 2013) and the original sampling forms in the Groningen Isotope Laboratory. Therefore, we adopted a relatively large vertical error on all Woldring *et al.* (2005) samples.

Kiden and Vos (2012)

Four samples were collected in the second half of the 1990s for geological mapping of the coastal area of the northern Netherlands. The dating results were used in the preliminary data evaluation and relative MSL reconstruction of Kiden and Vos (2012) but have not been published in internal reports of the Geological Survey or elsewhere.

CIO archives and RGD reports

The archives of the CIO, where most of the radiocarbon analyses in the Netherlands have been carried out, were carefully searched and analysed for all possible suitable samples. The records were searched for basal peat resting directly on Pleistocene sediments. Samples without location or with missing or unclear vertical position information were discarded. When samples were found to have potential, a literature search was carried out to see if the samples were already published. This included both the international scientific literature as well as reports from the Rijks Geologische Dienst (RGD): Dutch Geological Survey. If already published, we refer to the first citation of the sample in Table 1. In total, 14 previously unpublished basal peat samples were identified. Two were taken from a single offshore core from the North Sea. In some cases, the vertical position was reconstructed using the coordinates and high-resolution LIDAR data (AHN2; Van der Zon, 2013). We incorporated a large vertical error for these samples (see Supporting Information, Table S1).

Miscellaneous

Sample 34 was a basal peat sample taken from the Heveskesklooster megalithic tomb (Bakker, 1992; Cappers, 1993/1994), erected on coversands of periglacial origin and overgrown by peat during the Holocene. One additional sample (No. 19) was taken by the authors in 2013 at an excavation near Noordhorn, which was carefully levelled to a reliable LIDAR data benchmark position nearby.

Accuracy and error treatment

Age errors

Standard deviations of the dated radiocarbon samples were provided by the laboratory and were used to determine age errors (e.g. Kiden, 1995; Berendsen *et al.*, 2007). A 2σ cal a BP age range was used in this paper. In some cases, bulk peat samples may yield erroneous ^{14}C ages that are younger or older than the real age of the sample, due to introduction of younger or older carbon during or after peat formation (Törnqvist *et al.*, 1992). During peat growth, old organic matter may be incorporated in the peat in the form of infiltrated soil components or fragments of eroded and reworked older peat. After peat formation, younger organic matter may be admixed as a result of infiltration by humic acids, root penetration or bioturbation. We refer to Mook and Van de Plassche (1986) for a comprehensive overview of these and other factors which may contribute to incorrect ^{14}C ages of bulk peat samples. In a comparative study between conventional bulk and AMS samples, Berendsen *et al.* (2007) found no significant systematic differences in basal peat samples from the western Netherlands.

We did not consider reservoir effects. These would have been caused by non-atmospheric carbon, which in this case means the presence of aquatic plants in the peat samples. There are no indications for that in our basal peat samples.

Altitude errors

Vertical uncertainties of radiocarbon peat samples can be attributed to several different processes (Berendsen *et al.*, 2007; Hijma *et al.*, 2015). Firstly, different peat types develop at different local average water levels. Fen, reed and reed-sedge peat are assumed to form around 10 cm below the local water table (Berendsen *et al.*, 2007; Van de Plassche *et al.*, 2010). Wood peat forms at $\pm$10 cm around the local water table (Kiden, 1995; Törnqvist *et al.*, 1998; Van de Plassche *et al.*, 2005). For most of the dated samples in this study we do not have detailed information on peat composition, so we adopted a 20-cm error margin to account for the different peat types as suggested by Berendsen *et al.* (2007).

Secondly, compaction of sediments underlying basal peats can cause vertical displacement of samples (Hijma *et al.*, 2015). In our case, compaction of the Pleistocene base is negligible because of the relatively coarse clastic sediments (Jelgersma, 1961; Berendsen *et al.*, 2007). Moreover, we have only used samples of the base of the basal peat directly at the contact with the Pleistocene base. No samples from peat layers intercalated within the Holocene sedimentary sequence were used, except for the samples from De Jong (1984) and De Groot *et al.* (1996), which are detailed in the section 'data sets'. Therefore, we assume that our samples are not affected by compaction and no error calculations were deemed necessary.

Thirdly, the sample thickness introduces certain errors. Often, the samples are a couple of centimetres thick, which means there is an age difference between top and bottom, but also some compaction within the sample (Shennan,

1986). We treated these effects as vertical errors and we followed the assumption by Berendsen *et al.* (2007) that errors related to sample depth are generally <2 cm. Where the sample thickness was not known, we assumed that the given depth represented the centre of the sample. In addition, we used a sample thickness of 4 cm in the error calculations. We did not include errors for core stretching/shortening (Morton and White, 1997) or non-vertical drilling (Törnqvist *et al.*, 2004) as we expected them to be negligible.

Fourthly, elevation measurements include errors. In our case, the elevation of all sites was measured, which excludes possible vegetation zone errors (e.g. Goodbred *et al.*, 1998). If borehole altitudes were levelled relative to NAP benchmarks, errors should be smaller than 1 cm relative to NAP (Berendsen *et al.*, 2007). However, the method of levelling was not always recorded. In most cases, levelling to local benchmarks is assumed and we applied a vertical error of ±10 cm, corresponding with Engelhart (2010) and following the suggestion by Hijma *et al.* (2015). When levelling to NAP benchmarks did not take place, or altitude information was retrieved from other sources (digital elevation model, topographic maps) by the original authors, we used an error margin of ±50 cm, corresponding with Hijma *et al.* (2015). For offshore boreholes, a vertical tidal error has to be taken into account. Shennan (1986) suggests assigning an error of half a tidal range. Kiden *et al.* (2002) and Vink *et al.* (2007), for example, assigned these samples an altitude accuracy of ±1.0 m, which we also adopt in this paper. This corresponds well with North Sea coast reference values showing a tidal range of 167 cm in the west of the study area (island of Texel; Fig. 3) to 218 cm (island of Schiermonnikoog) in the east (Rijkswaterstaat, 2011). The error calculations are presented in Supporting Information, Table S1.

The total vertical uncertainty or error e_h (m) was calculated as (Shennan *et al.*, 2006; Hijma *et al.*, 2015):

$$e_h = \sqrt{({e_{\text{law}}}^2 + {e_{\text{comp}}}^2 + {e_{\text{d}}}^2 + {e_{\text{NAP}}}^2)}$$

where: e_{law} = local average water level uncertainty (m); e_{comp} = compaction uncertainty (m); e_{d} = sample thickness uncertainty (m); and e_{NAP} = benchmark uncertainty (m).

Although vertical uncertainty is not a statistically determined error, some authors (e.g. Hijma and Cohen, 2010) interpret e_h as a 1σ error, which we also adopt here. After vertical error and radiocarbon age determination, the radiocarbon age samples (Table 1) were plotted in a time–depth diagram including the horizontal 2σ age range and the vertical error e_h.

Sea-level reconstruction

We fit the data with an empirical hierarchical model (e.g. Kopp *et al.*, 2016) to reconstruct the relative MSL for the Wadden Sea and to be able to distinguish between the Wadden Sea and western Netherlands regions. The model divides into a data level, a process level and a hyperparameter level. At the data level, index points are treated as noisy measurements of the underlying sea-level field, with vertical measurement and indicative range errors assumed to be uncorrelated and normally distributed, and geochronological errors approximated as uncorrelated and normally distributed. As in Kopp *et al.* (2016), geochronological uncertainties are approximated using the Noisy Input Gaussian Process methodology of McHutchon and Rasmussen (2011). At the process level, relative MSL $f_i(t)$ at each site i is modelled as the sum of two terms, each with Gaussian process priors (Rasmussen and Williams, 2006). The first term, $g(t)$, represents a non-linear signal common to both sites, while the second term, $m_i(t)$, represents a slowly varying, region-specific non-linear signal:

$$f_i(t) = g(t) + m_i(t)$$

The priors for each of the terms are characterized by hyperparameters, which capture *a priori* expectations about characteristics such as the variability of the term and the timescale of variation of the term. The priors for $g(t)$ and $m_i(t)$ have once-differentiable, Matérn-3/2 covariance functions. In an empirical model, the hyperparameters are optimized to maximize the likelihood of the model given the data. For $g(t)$, the prior standard deviation is 29.9 m and the time scale is 13.2 kyr; for $m_i(t)$, the prior standard deviation is 0.8 m and the time scale is 0.6 kyr.

Conditioning the model upon the data yields a mean posterior estimate of relative MSL at each site over time, as well as an associated spatiotemporal covariance matrix. Linear transformation of the mean and of the covariance matrix yields an estimate of the inter-site differences and their associated uncertainties. As modelling input, we used the Hijma and Cohen (2010) and Berendsen *et al.* (2007) data for the western Netherlands in combination with the index points from the Wadden Sea as presented in this study.

Results

Sea-level index points

All 51 radiocarbon samples available for the Wadden Sea area were plotted in a time–depth diagram. The distribution of the samples shows a sharp lower boundary and an indistinct upper limit. Based on the criteria described in the methodology section, 26 samples were regarded as suitable index points for relative MSL reconstruction. Twenty-five samples were excluded (Fig. 5).

Relative mean sea-level reconstruction

The modelled relative MSL curve for the Wadden Sea is presented with a 2σ error band in Fig. 6. The curve shows a sharp rise from 8200 to 7500 cal a BP of 7.3 ± 0.6 m (1σ) in this period, a rate of 10.4 ± 0.9 mm a^{-1} (1σ). After this period the rate decreases to 3.5 ± 0.3 mm a^{-1} between 7500 and 6000 cal a BP. From 6000 to 4500 cal a BP, the relative MSL rises by 2.4 ± 0.8 m, an average rate of 1.6 ± 0.5 mm a^{-1}. From 4500 to 2500 cal a BP the total relative MSL rise was 1.6 ± 0.8 m, an average rate of 0.8 ± 0.4 mm a^{-1}. The vertical error band is relatively wide in this section due to a limited number of suitable data points. After 2500 cal a BP until the youngest sample at about 600 cal a BP, the sea level rise appears to be linear at 0.6 ± 0.3 mm a^{-1}, but the peat samples chosen here probably reflect a groundwater level slightly higher than MSL, which is discussed in more detail in the Regional differences section.

Interpretation

A new relative MSL curve for the Dutch Wadden Sea

When reconstructing relative MSL changes for a single region, differential isostatic rebound and locally varying coastal

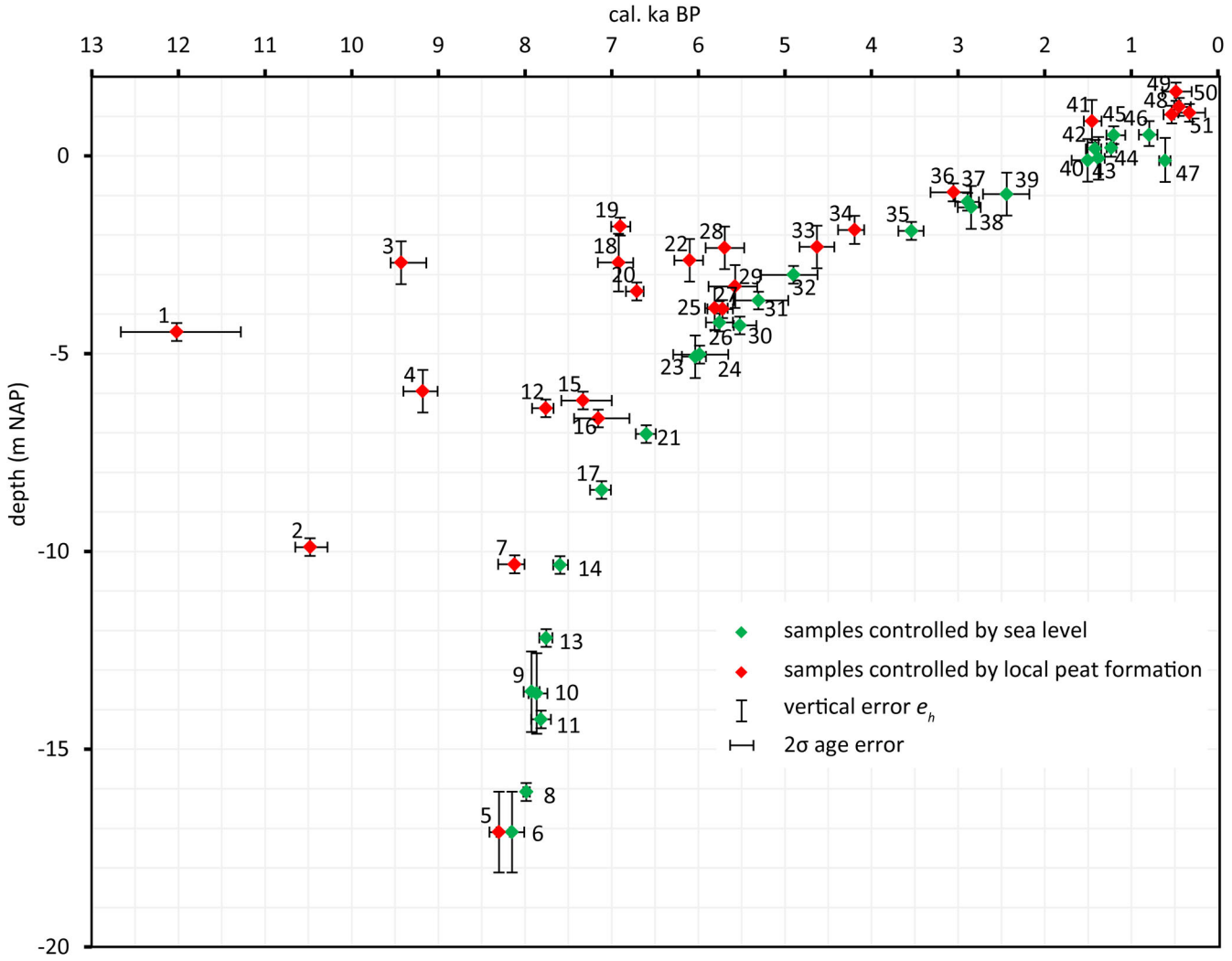

Figure 5. Time–depth diagram of all available radiocarbon-dated basal peat samples. Numbers refer to Table 1.

configurations necessitate that the study area should not be too large (Kiden *et al.*, 2002; Bungenstock and Weerts, 2010) and care should be taken in areas with diverse coastal settings (Baeteman *et al.*, 2011).

To avoid the effects of differential isostatic movements within the study area itself, Kiden *et al.* (2002) suggested a maximum size of *ca.* 50 by 50 km as a rule of thumb. In our study area, we could expect some differential movements due to the size of the area (150 km). As the study area is orientated west to east, it is situated at a 45° angle relative to the direction of subsidence (SW–NE, see *e.g.* Kiden *et al.*, 2002; Vink *et al.*, 2007), and thus it measures roughly 100 km in the direction of maximal subsidence.

The maximum extent of a study area also depends on the coastal configuration (Baeteman *et al.*, 2011). In the Wadden Sea region, tidal basins exhibit a very dynamic behaviour throughout the Holocene, as shown by Baeteman *et al.* (2011), Bazelmans *et al.* (2011) and Vos (2015). The Wadden Sea area includes intertidal channels and shoals, but also barrier islands (Frisian Islands) separated by major tidal inlets and ebb-tidal deltas. The (undiked) tidal marshes on the mainland are also included (Oost, 1995; Oost *et al.*, 2012). The palaeo-geographical map series by Vos and De Vries (2015) (Fig. 7) show the varying size of the basin through time, but also indicate that from a geomorphological view it can be regarded as a single entity. Although the area is relatively large in respect to the size suggested by Kiden *et al.* (2002), we hypothesize that, from a sea-level reconstruction point of view, it can be regarded to a first approximation as a single entity. To test the hypothesis, we have split the data into a western and an eastern dataset to check for differences in the relative MSL curves.

The Pleistocene subsurface includes four relatively small valleys/tidal basins (the Boorne, Hunze, Fivel and Ems-Dollard; Vos, 2015). We placed the dividing line between the two subsets on the Pleistocene high between the Boorne and Hunze tidal basins (Fig. 8), thereby separating the western Wadden Sea (i.e. Boorne tidal basin) from the eastern Wadden Sea (i.e. Hunze and Fivel tidal basin and Ems-Dollard estuary; Fig. 7).

By plotting the samples in a time–depth diagram (Fig. 9), it transpires that the index points from both subsets are on a single curve. During the periods 6000–5000 cal a BP and 3000–1000 cal a BP the two curves coincide. The centroids of the index points may show some deviations older than 7700 cal a BP, but the error bars overlap to a great extent. Although for the periods 7700–5500 cal a BP and 5000–3000 cal a BP no index points of the western Wadden Sea are present in our dataset, we conclude that based on the currently available data there is no reason to differentiate the relative MSL histories of the eastern and western Dutch Wadden Sea.

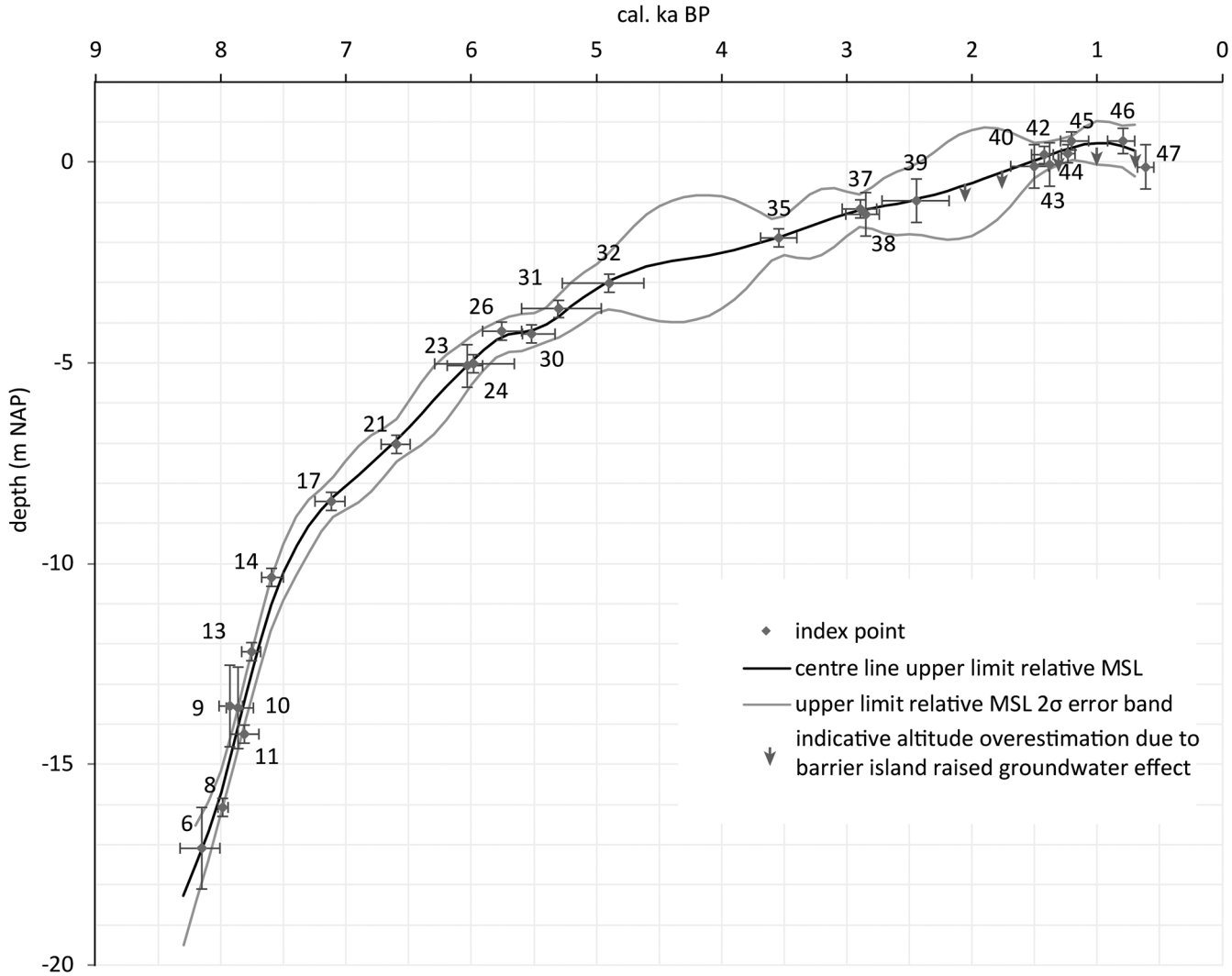

Figure 6. Relative MSL reconstruction for the Wadden Sea region. The barrier island raised groundwater effect is discussed in the Regional differences section.

Regional differences

When comparing the Wadden Sea curve to curves from neighbouring areas (Fig. 10), it is clear that the Wadden Sea curve has a considerably lower time–depth position than the curves for Belgium (Denys and Baeteman, 1995) and Zeeland (south-western Netherlands; Kiden, 1995; Vink *et al.*, 2007). The vertical difference ranges from 4 to 6 m lower around 8000 cal a BP decreasing to 2 m around 6000 cal a BP, and the Belgium and Zeeland error bands are outside of the error band of the Wadden Sea curve. Between 5000 and 4000 cal a BP the Zeeland centre line reaches the upper limit of the Wadden Sea upper 2σ error band.

Compared to the western Netherlands curves (Hijma and Cohen, 2010; Van de Plassche *et al.*, 2010), between 8200 and 6400 cal a BP, the time–depth position of the Wadden Sea curve (Fig. 11a) is significantly lower than the western Netherlands curve (probability $p > 0.86$; $p > 0.95$ for all time points before 7100 BP; Supporting Information S2). For the steepest section between 8200 and 7500 cal a BP, average relative MSL rise rates are 10.4 ± 0.9 mm a^{-1} (1σ) for the Wadden Sea and 7.7 ± 0.5 mm a^{-1} for the western Netherlands. After 6400 cal a BP, the two curves are almost always indistinguishable within uncertainty (Fig. 11b). The similarity between this younger part of the two curves agrees with the suggestion of Van de Plassche (1982) that there is no significant difference between the relative MSL curve of the western Netherlands and the Wadden Sea for this period. The average relative MSL rise rate of 1.6 ± 0.5 mm a^{-1} shown in the Wadden Sea curve is not significantly different from the rise of around 1.7 ± 0.2 mm a^{-1} for the western Netherlands curve in the period 6000–4500 cal a BP. The steady rise in RSL of 0.78 ± 0.4 mm a^{-1} between 4500 cal a BP and 2500 cal a BP also appears comparable to the 0.6 ± 1.3 mm a^{-1} rise for the western Netherlands.

In comparison to the Central Netherlands (Van de Plassche *et al.*, 2005), our Wadden Sea reconstruction is slightly higher. The Central Netherlands curve is within the 2σ error band for most of its trajectory, however.

For the period 1750–1000 cal a BP, the Wadden Sea curve centre line fluctuates around the upper MHW limit of the curve for the Frisian Islands constructed by De Groot *et al.* (1996) (Fig. 10). Although the latter was based on sedimentary structures, and peat samples were used for uncertainty analysis, the relative MSL rise rate is similar to our Wadden Sea curve (1.0 ± 0.3 mm a^{-1} for the period 2500–1000 cal a BP). It needs to be noted, however, that the peat samples chosen for our Wadden Sea curve here probably reflect a groundwater level slightly higher than mean sea level. This may be explained by the barrier island raised groundwater effect or Ghijben-Herzberg principle, which is based on the density differences between salt and fresh water

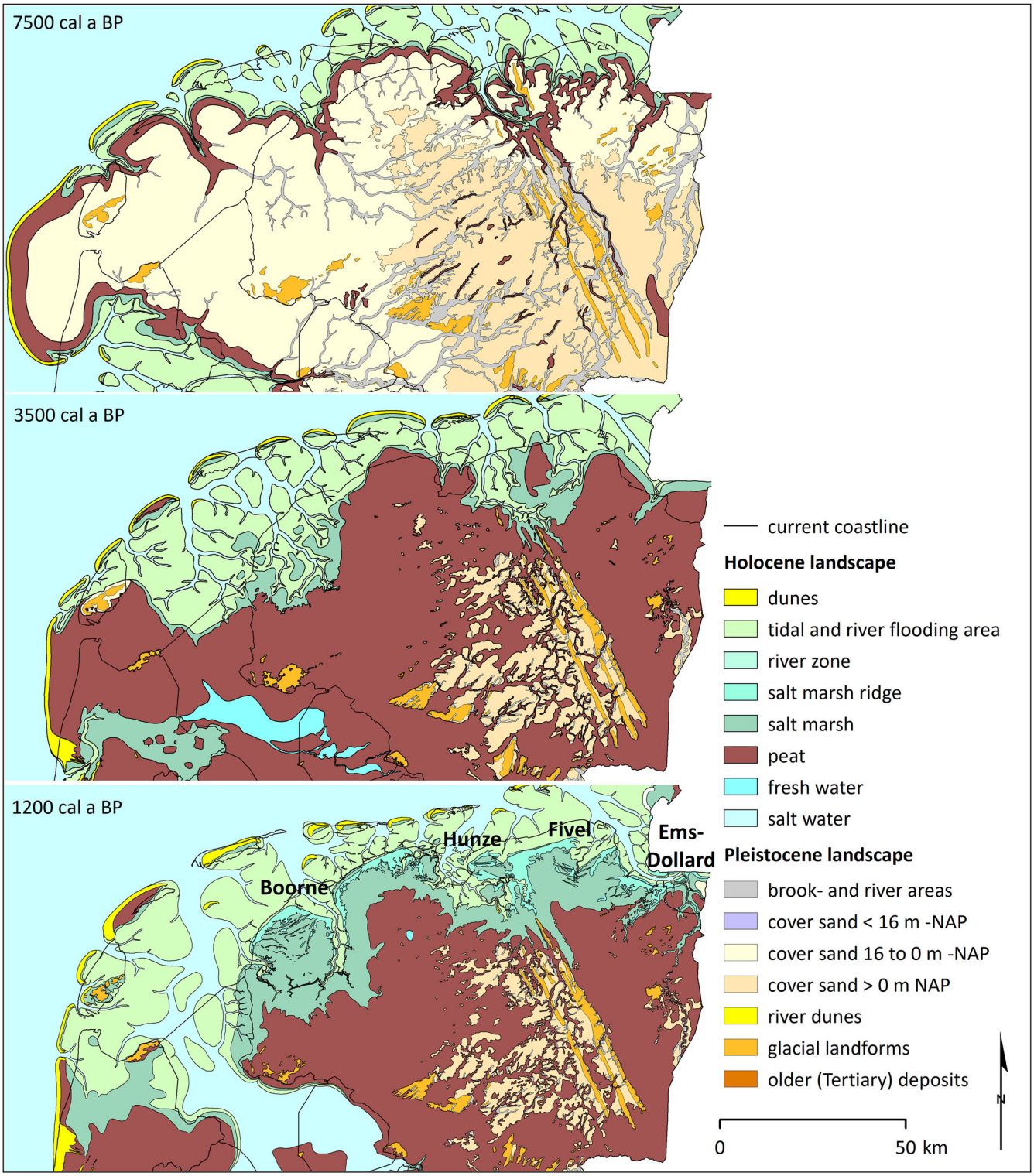

Figure 7. Palaeogeographical maps of the Wadden Sea area (Vos and De Vries, 2015).

(Drabbe and Badon Ghijben, 1889; Herzberg, 1901). The fresh groundwater table is elevated above sea level in coastal dunes and on barrier islands such as those in the Wadden Sea (Grootjans *et al.*, 1996; Röper *et al.*, 2012). The elevation of the groundwater table depends on the depth and extent of the freshwater lens on the island. In the Frisian Islands, raised groundwater levels of over 2 m above relative MSL have been measured on Spiekeroog in Germany (Tronicke *et al.*, 1999) and 3.5 m above relative MSL on the Dutch island of Schiermonnikoog (Grootjans *et al.*, 1996). This means that on Wadden islands, peat samples indicate higher groundwater levels, which would imply that such peat samples need to be considered as upper limit indicators. Therefore, the younger section of the relative MSL curve should probably be lower than our Wadden Sea reconstruction, which is indicatively shown by the red arrows in Figs 6, 10, 11a and 12.

GIA-induced crustal movements

As discussed above, the new relative MSL reconstruction for the northern Netherlands is below the curves for Belgium

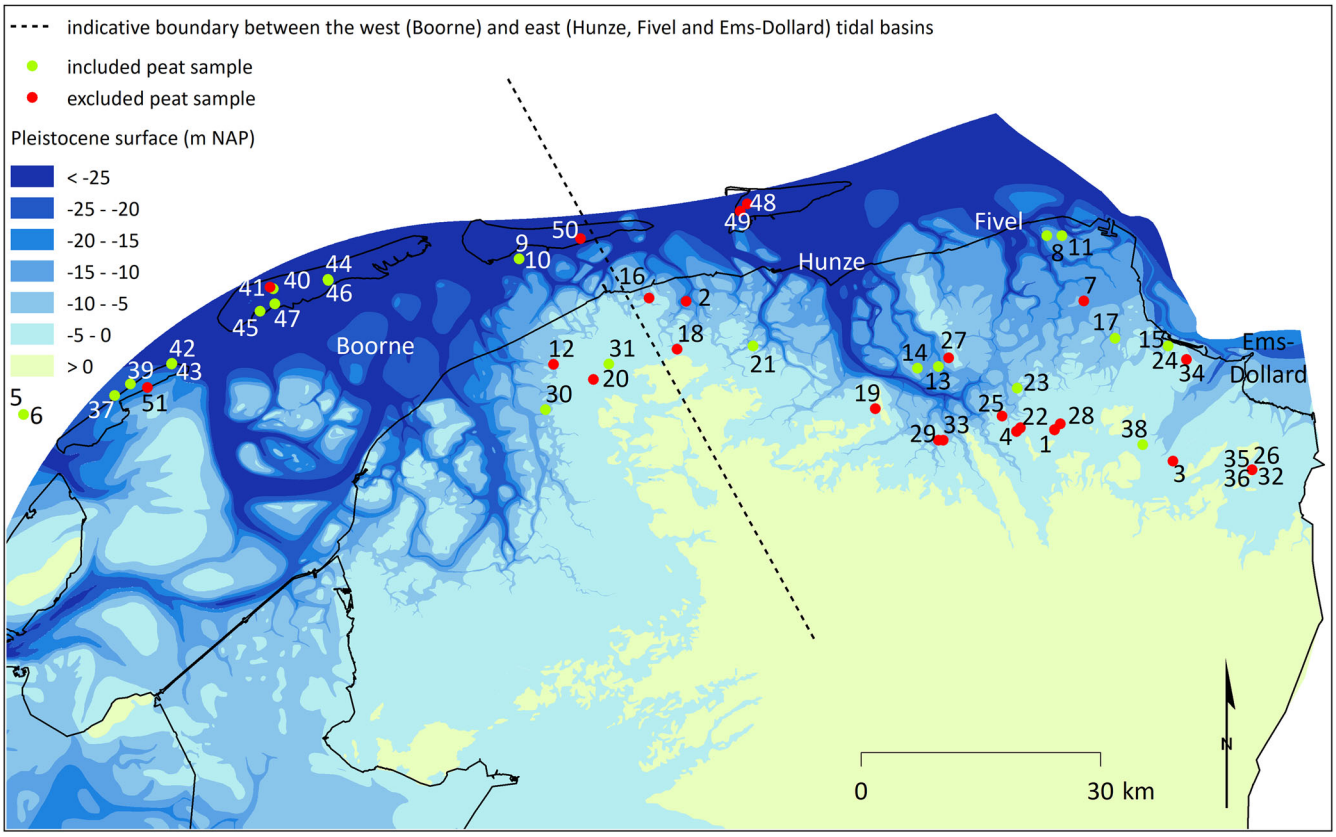

Figure 8. Top of the Pleistocene substratum (Vos and De Vries, 2015) with sample locations.

and the south-western Netherlands, in accordance with the hypothesis of increasing isostatic subsidence towards the north. Here we further compare our Wadden Sea curve with relative MSL predictions from existing geodynamic earth models.

Vink *et al.* (2007) present relative MSL predictions for several sites in the southern North Sea, based on a regional best-fit geodynamic earth model that incorporates glacio- and hydro-isostatic vertical crustal movements. Relevant here are their predictions for Den Helder and Winschoten in the extreme west and east of our Wadden Sea study area, respectively (Fig. 3). Crustal movements in the Netherlands also contain a tectonic component, but in the early and middle Holocene in particular it is considerably smaller than the glacio-hydro-isostatic component (Kiden *et al.*, 2002, 2008). We will therefore focus here on the GIA-induced crustal movements as predicted by the geodynamic earth models.

Figure 12 shows the western Netherlands and Wadden Sea area relative MSL predictions from Vink *et al.* (2007) together with the relative MSL curve for the western Netherlands (Hijma and Cohen, 2010) and the Wadden Sea error band presented here. The Wadden Sea error band is always above the Wadden Sea GIA model predictions, but its oldest part around 8000 cal a BP is only 1–2 m higher. This reasonably good correspondence between observations and model results at this early date subsequently deteriorates: at 7500 cal a BP, the Wadden Sea error band is 2.5–3.7 m higher than the RSL predictions for Den Helder and Winschoten, respectively. At around 6500 cal a BP, there is a conspicuous high 'shoulder' in the predicted relative MSL curves for both the Wadden Sea area and the western Netherlands, temporally reducing the difference between the observations and the predictions for Den Helder to a minimum of around 0.4 m. It is striking, however, that at this date the relative MSL predictions for the western Netherlands plot about 1.5 m higher than the well-established relative MSL curve of that region based on actual data [see also review of the relative MSL error band of Van de Plassche and Roep (1989) in Kiden *et al.* (2002)]. This casts some doubt on the reliability of the model for the western Netherlands and possibly also for the Wadden Sea area around 6500 cal a BP. After 6000 cal BP, the Wadden Sea curve is again substantially higher than both relative MSL predictions for the Wadden Sea region, with the difference decreasing slightly from 1.2–1.8 m at 6000 cal a BP to 1.1–1.4 m at 3000 cal a BP.

Discussion, conclusions and recommendations

There are enough data to reliably reconstruct a curve representing the upper limit of relative MSL rise for the Wadden Sea area for the period from 8200 to 2500 cal a BP. The number of suitable index points has now been expanded to a total of 51 dates from the base of the basal peat, of which 26 are argued to be suitable proxies for relative MSL.

With respect to regional differences in relative MSL for the period before 6400 cal a BP, we confirm that the Wadden Sea curve is situated below the MSL reconstructions for Belgium (Denys and Baeteman, 1995), Zeeland (Kiden, 1995) and the western Netherlands (Hijma and Cohen, 2010; Van de Plassche *et al.*, 2010). The oldest/deepest part of the curve is also in reasonable agreement with glacio-isostatic modelling results, supporting the hypothesis that the Wadden Sea is closer to the zone of maximal postglacial subsidence.

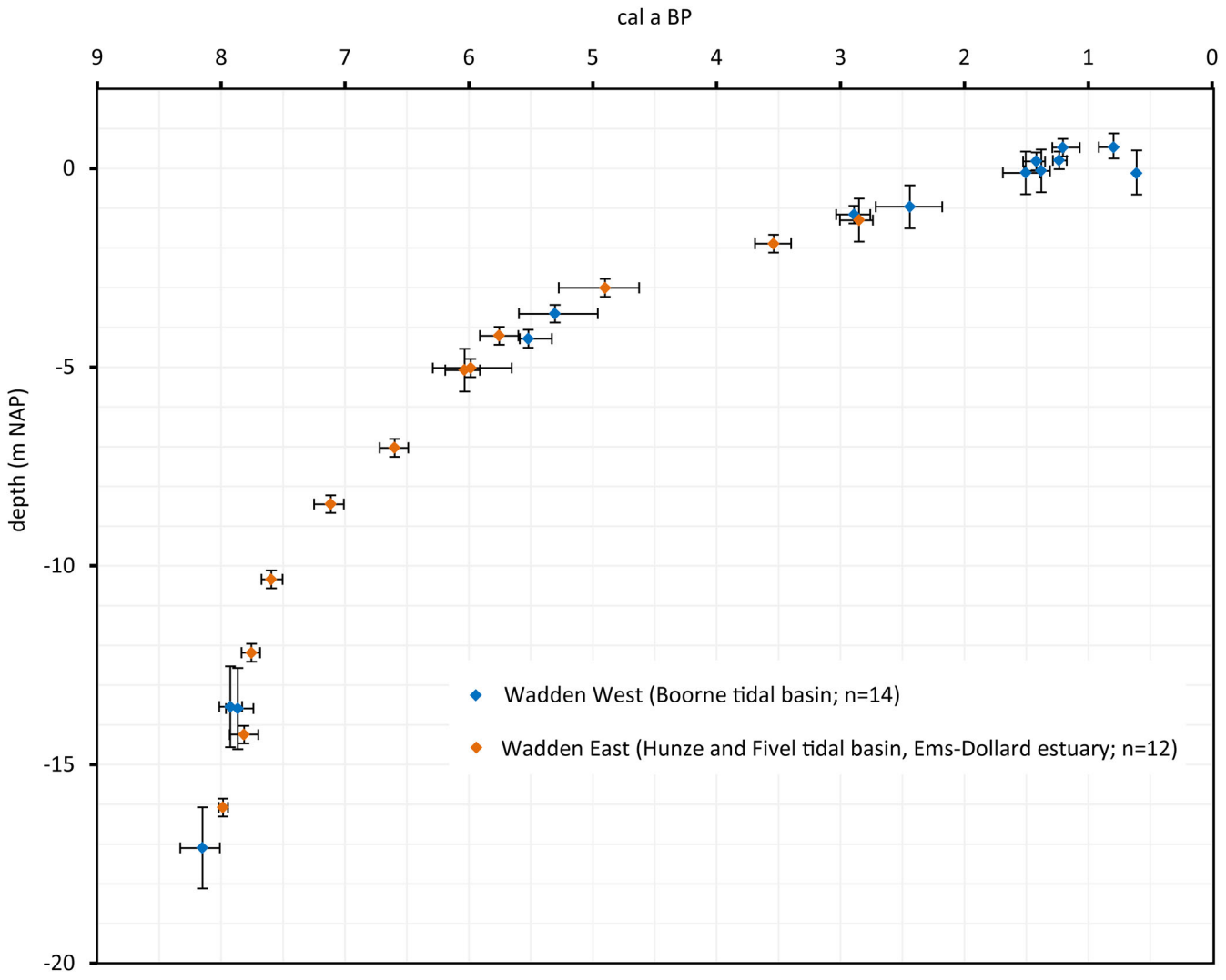

Figure 9. Wadden Sea index points split into a western and eastern section.

For the period after 6400 cal a BP, however, the Wadden Sea curve shows no significant difference with the Hijma and Cohen (2010) and Van de Plassche *et al.* (2005, 2010) relative MSL reconstructions for the western and central Netherlands. It also is higher than relative MSL predictions from GIA models. This apparently supports the idea of Van de Plassche (1982) that these younger parts of the western and northern Netherlands relative MSL histories are the same. However, the presently available data set of basal peat dates provides information on local groundwater levels which in the best case are at or very close to relative MSL but may be higher than relative MSL as well. Therefore, the actual sea-level curve for the Wadden Sea area could be below the reconstruction presented here and thus also below relative MSL in the western Netherlands. This can only be confirmed when more data become available with a density that is comparable to the western Netherlands. The current data set available to us for the period 6400–2500 cal a BP cannot (yet) be used to conclusively confirm or reject the hypothesis that the relative MSL histories of the northern and western Netherlands are similar.

Assuming that the data are representative of the true course of Holocene sea-level in the region would imply that the GIA model predictions are only 1–2 m lower than the relative MSL reconstruction at *ca.* 8000 cal a BP while at about 7500 cal a BP they underestimate sea-level by 2.5 to almost 4 m. Although around 6500 cal a BP the difference between the model predictions and the Wadden Sea curve is somewhat less, the discrepancy increases again to 1.5 m around 6000 cal a BP and then decreases slowly towards the present. If real, the significance of this observation in terms of postglacial peripheral bulge collapse is as yet unclear but warrants further study from both sea-level data quality/reliability and GIA-modelling points of view.

The currently presented Wadden Sea reconstruction may be somewhat too high from 2500 to 1000 cal a BP, as peat growth on barrier islands may be influenced by fresh groundwater being pushed up by deeper salt water, typical for Frisian Islands. In addition, for the most recent period (2000–500 cal a BP), we have used basal peats lying on sandy Holocene marine deposits. Although they appear to be relatively stable based on the core descriptions, we cannot fully assess possible compaction problems.

Changes in palaeotidal range could have affected the shape of the North Sea sea-level curve. For example, tides in the North Atlantic Ocean were amplified around 9000 cal a BP, due to opening of the Hudson Strait (Hill *et al.*, 2011). In the North Sea region, the amplification was completed by 7000 cal a BP when the North Sea and

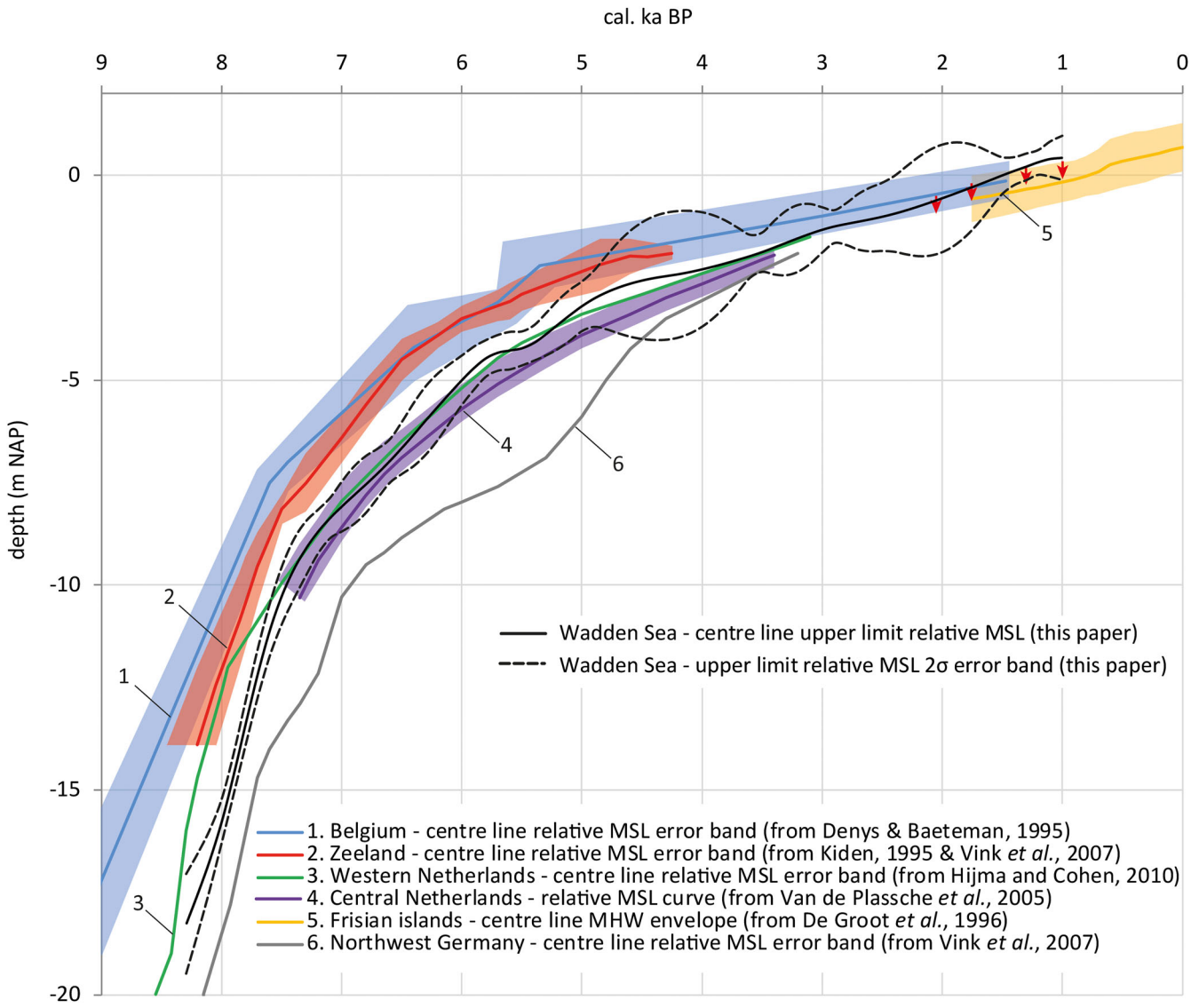

Figure 10. Holocene relative MSL error band for the Dutch Wadden Sea combined with regional curves from neighbouring areas.

Southern Bight became fully connected (Van der Molen and de Swart, 2001; Uehara *et al.*, 2006; Hijma and Cohen, 2010). Correcting regional sea-level reconstructions for these changes in palaeotidal range remains an area for further study.

Despite the limitations and caveats mentioned above, the Holocene relative MSL reconstruction for the northern Netherlands presented here should be considered a reliable first assessment of the best data currently available, to be expanded and improved upon by new data acquired explicitly for sea-level reconstruction. For a more definitive answer to the question of whether the relative MSL curve for the northern Netherlands is similar to, or different from, that of the western Netherlands, or whether the GIA models are in error and to what extent, we recommend a more detailed regional field campaign. Reliable basal peat samples would preferably come from areas with a steep non-eroded Pleistocene subsurface, minimizing the effect of local groundwater levels on basal peat growth.

There is scope to improve data coverage for the late Holocene. It would be useful to combine sedimentological data from below dune-lees and man-made terps and use archaeological evidence for age control and as indicator of inundation frequencies. Sea level research like that of De Groot *et al.* (1996) on the Wadden islands during the last 2000 years and that of Nieuwhof and Vos (2018) using MHW index points from beneath man-made terps show promising results to bridge the gap between instrumental records (e.g. tide gauges) and palaeo-observation-based reconstructions (Vermeersen *et al.*, accepted).

Our reconstruction might be improved further by incorporating types of dates other than from basal peats. Such improvements may include the use of salt marsh microfossil analyses, especially diatoms and testate amoebae (Barlow *et al.*, 2013), as foraminifera are very rare in Dutch coastal deposits. Although the salt marshes of the mainland have been diked since around 1100 ad, the salt marsh deposits on the back-barrier side of the islands are still open to marine influences and may cover the last 700 years, which also creates the possibility to improve the more recent part of the RSL reconstruction.

Misfits between GIA models and data will always remain because GIA modelling cannot provide unique solutions around the globe. Earth parameters rely on thickness and type of lithosphere and will differ from region to region.

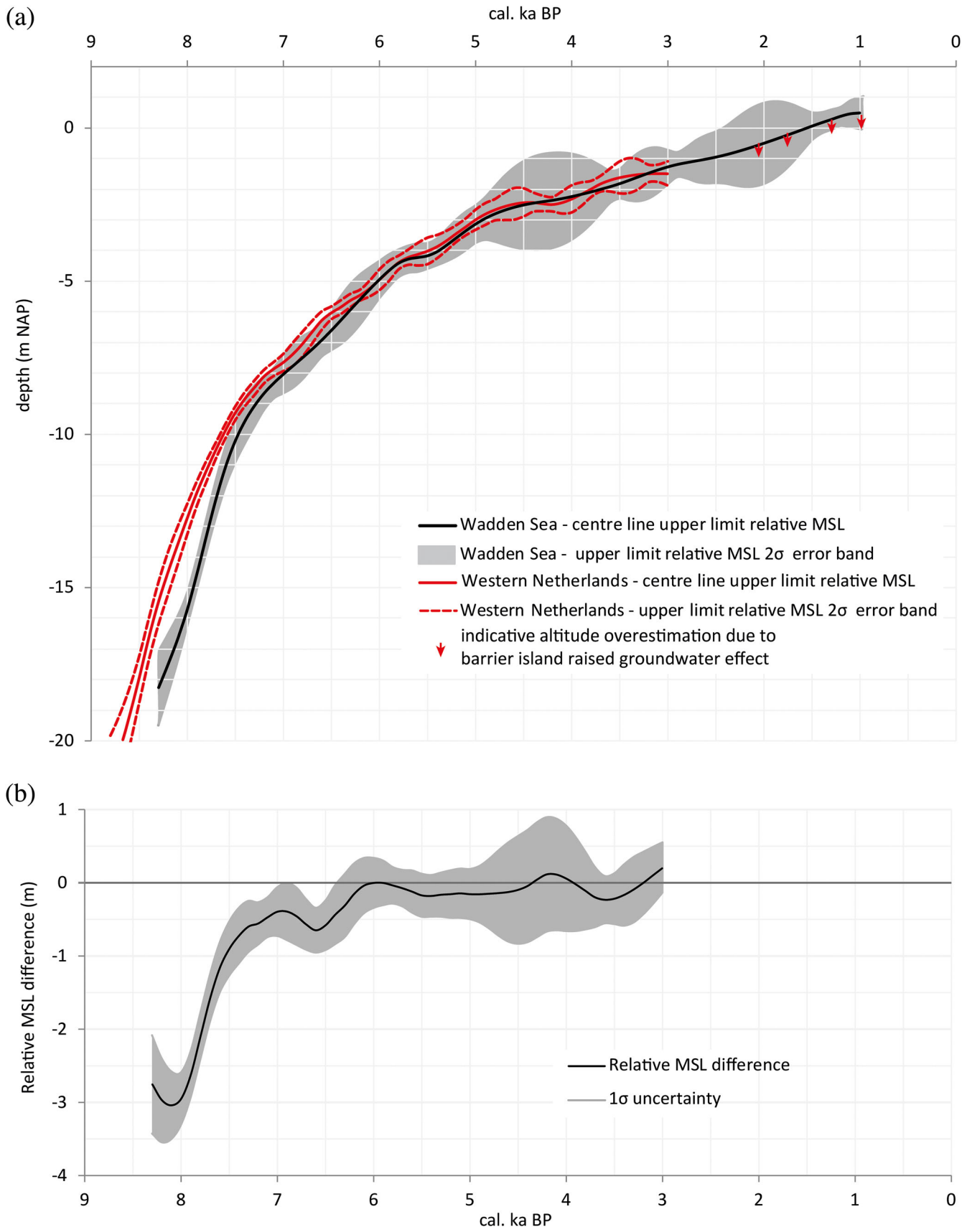

Figure 11. The Wadden Sea and Western Netherlands relative MSL reconstructions plotted in a time depth diagram (a) and as relative MSL difference (b; Wadden Sea minus western Netherlands).

Nonetheless, by refining GIA models and by improving data quality and coverage, improvements can be made in the reconstruction of past ice-sheet changes and determination of Earth rheological properties (Whitehouse, 2018). New data, such as those provided in this study, will go some way to better understand global GIA processes as a component of current and future ice-sheet and sea-level change.

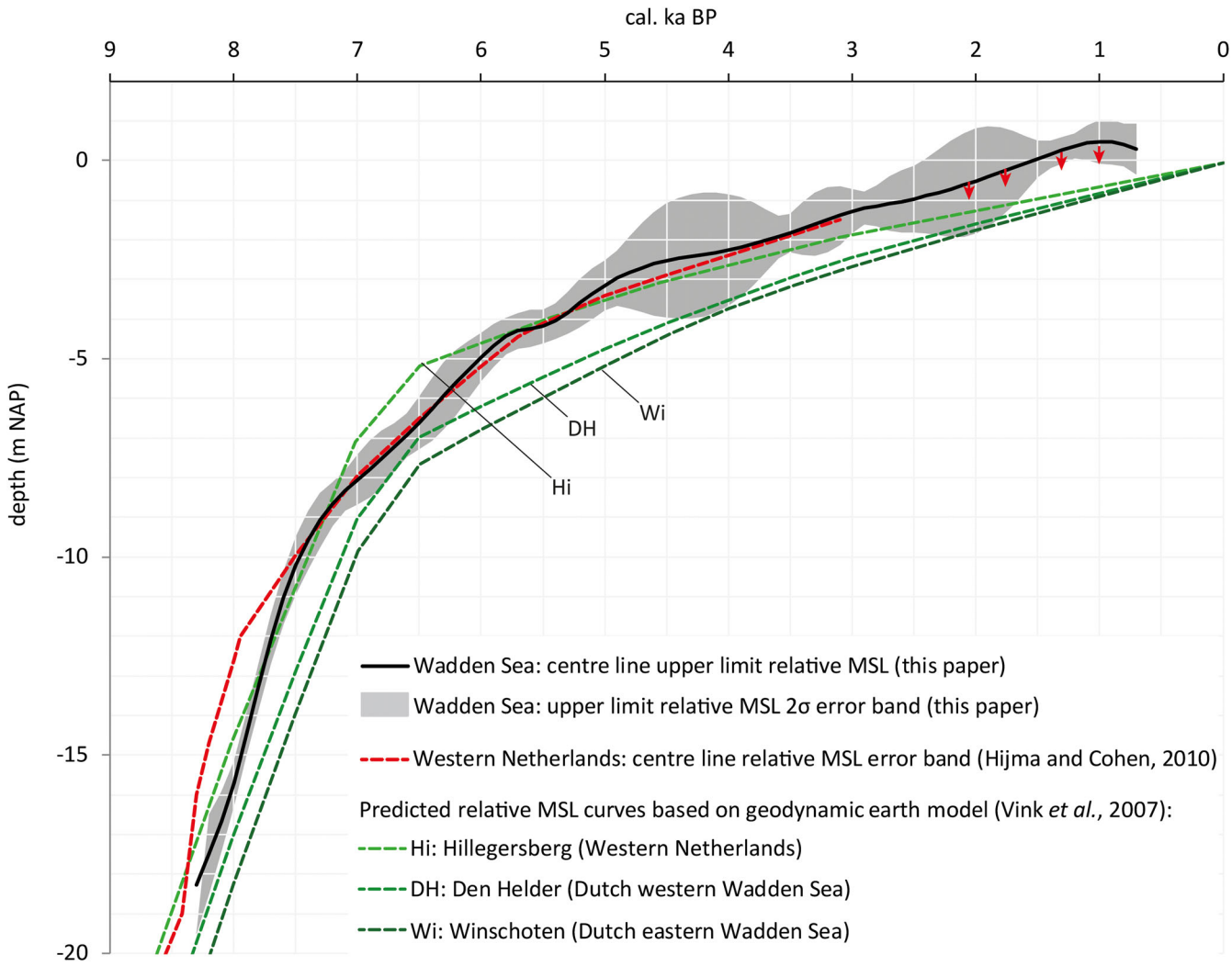

Figure 12. Reconstructed Wadden Sea curve from this study compared to the GIA model predictions of Vink *et al.* (2007).

Supporting Information

S1. Full data table.
S2. Model results.

Abbreviations. AMS, accelerator mass spectrometry; GIA, glacial isostatic adjustment; MHW, mean high water level; MSL, mean sea level; NAP, Dutch Ordnance Datum; RSL, relative sea level; SLIPs, sea level index points.

References

Baeteman C, Waller M, Kiden P. 2011. Reconstructing middle to late Holocene sea-level change: a methodological review with particular reference to 'A new Holocene sea-level curve for the southern North Sea' presented by K-E Behre. *Boreas* **40**: 557–572.

Baeteman C, Waller M, Kiden P. 2012. 'Reconstructing middle to late Holocene sea-level change: A methodological review with particular reference to "A new Holocene sea-level curve for the southern North Sea" presented by K.-E. Behre': Reply to comments. *Boreas* **41**: 315–318.

Bakker JA. 1992. *The Dutch Hunebedden: Megalithic Tombs of the Funnel Beaker Culture. Archaeological Series/International Monographs in Prehistory* Vol. 2. Oxford: Oxbow Books.

Bard E, Hamelin B, Arnold M *et al.* 1996. Deglacial sea-level record from Tahiti corals and the timing of global meltwater discharge. *Nature* **382**: 241–244.

Barlow NLM, Shennan I, Long AJ *et al.* 2013. Salt marshes as late Holocene tide gauges. *Global and Planetary Change* **106**: 90–110.

Bazelmans J, Meier D, Nieuwhof A *et al.* 2012. Understanding the cultural historical value of the Wadden Sea region. The co-evolution of environment and society in the Wadden Sea area in the Holocene up until early modern times (11,700 BC −1800 AD): an outline. *Ocean & Coastal Management* **68**: 114–126.

Bazelmans J, Van der Meulen M, Weerts H *et al.* 2011. *Atlas Van Nederland in Het Holoceen*. Amsterdam: Bert Bakker.

Beets DJ, Van der Spek AJF. 2000. The Holocene evolution of the barrier and the back-barrier basins of Belgium and the Netherlands as a function of late Weichselian morphology, relative sea-level rise and sediment supply. *Netherlands Journal of Geosciences* **79**: 3–16.

Behre KE. 2007. A new Holocene sea-level curve for the southern North Sea. *Boreas* **36**: 82–102.

Behre KE. 2012a. Sea-level changes in the southern North Sea region: a response to Bungenstock and Weerts (2010). *International Journal of Earth Sciences* **101**: 1077–1082.

Behre KE. 2012b. 'Reconstructing middle to late Holocene sea-level change: a methodological review with particular reference to "A new Holocene sea-level curve for the southern North Sea" presented by K.-E. Behre': Comments. *Boreas* **41**: 308–314.

Bennema J. 1954. Bodem- en zeespiegelbewegingen in het Nederlandse kustgebied. *Boor en Spade* **7**: 1–96.

Berendsen HJA, Makaske B, Van de Plassche Ovd *et al.* 2007. New groundwater-level rise data from the Rhine-Meuse Delta – implications for the reconstruction of Holocene relative mean sea-level rise and differential land-level movements. *Netherlands Journal of Geosciences* **86**: 333–354.

Bronk Ramsey C. 1995. Radiocarbon calibration and analysis of stratigraphy: the OxCal program. *Radiocarbon* **37**: 425–430.

Bronk Ramsey C. 2001. Development of the radiocarbon calibration program. *Radiocarbon* **43**: 355–363.

Bungenstock F, Weerts HJT. 2010. The high-resolution Holocene sea-level curve for Northwest Germany: global signals, local effects or data-artefacts? *International Journal of Earth Sciences* **99**: 1687–1706.

Bungenstock F, Weerts HJT. 2012. Holocene relative sea-level curves for the German North sea coast. *International Journal of Earth Sciences* **101**: 1083–1090.

Cappers RTJ. 1993/4. Botanical macro-remains of vascular plants of the Heveskesklooster terp (the Netherlands) as tools to characterize the past environment. *Palaeohistorica* **35/36**: 107–167.

Cohen KM. 2005. 3D geostatistical interpolation and geological interpretation of palaeogroundwater rise in the coastal prism in the Netherlands. In *River Deltas: Concepts, Models, and Examples*, Giosan L, Bhattacharaya JP (eds). Tulsa: Society for Sedimentary Geology; 341–364.

Cook GT, Van der Plicht J. 2013. Radiocarbon dating – conventional method. In *Encyclopedia of Quaternary Science* 2nd edn, Elias S, Mock C (eds). Amsterdam: Elsevier; 305–315.

De Groot TAM, Westerhoff WE, Bosch JHA. 1996. Sea-level rise during the last 2000 years as recorded on the Frisian Islands (the Netherlands). *Mededelingen Rijks Geologische Dienst* **57**: 69–78.

De Jong J. 1984. Age and vegetational history of the coastal dunes in the Frisian Islands. *Geologie en Mijnbouw* **63**: 269–275.

De Vries Hd, Katsman C, Drijfhout S. 2014. Constructing scenarios of regional sea level change using global temperature pathways. *Environmental Research Letters* **9**: 115007.

Denys L, Baeteman C. 1995. Holocene evolution of relative sea level and local mean high water spring tides in Belgium – a first assessment. *Marine Geology* **124**: 1–19.

Drabbe J, Badon Ghijben W. 1889. Nota in verband met de voorgenomen putboring nabij Amsterdam. *Tijdschrift van Het Koninklijk Instituut van Ingenieurs, Verhandelingen* **1888/9**: 8–22.

Engelhart SE. 2010. *Sea-level changes along the U.S. Atlantic coast: implications for glacial isostatic adjustment models and current rates of sea-level change*. PhD Thesis, University of Pennsylvania.

Fairbanks RG. 1989. A 17,000-year glacio-eustatic sea level record: influence of glacial melting rates on the Younger Dryas event and deep-ocean circulation. *Nature* **342**: 637–642.

Gehrels WR. 2010. Late Holocene land- and sea-level changes in the British Isles: implications for future sea-level predictions. *Quaternary Science Reviews* **29**: 1648–1660.

Goodbred SL, Wright EE, Hine AC. 1998. Sea-level change and storm-surge deposition in a late Holocene Florida salt marsh. *Journal of Sedimentary Research* **68**: 240–252.

Griede JW. 1978. *Het ontstaan van Frieslands noordhoek. Een fysisch-geografisch onderzoek naar de Holocene ontwikkeling van een zeekleigebied*. PhD Dissertation, Free University Amsterdam.

Grootjans AP, Sival FP, Stuyfzand PJ. 1996. Hydro-geochemical analysis of a degraded dune slack. *Vegetatio* **126**: 27–38.

Herzberg A. 1901. Die Wasserversorgung einiger Nordseebäder. *Journal für Gasbeleuchtung und Wasserversorgung* **44**: 815–819; 842–844.

Hijma MP, Cohen KM. 2010. Timing and magnitude of the sea-level jump preluding the 8200 yr event. *Geology* **38**: 275–278.

Hijma MP, Engelhart SE, Törnqvist TEBP *et al.* 2015. A protocol for a geological sea-level database. In *Handbook of Sea-Level Research*, Shennan I, Long AJ, Horton BP (eds). Hoboken: John Wiley & Sons; 536–554.

Hill DF, Griffiths SD, Peltier WRBP *et al.* 2011. High-resolution numerical modeling of tides in the western Atlantic, Gulf of Mexico, and Caribbean Sea during the Holocene. *Journal of Geophysical Research* **116**: C10014.

Jelgersma S. 1961. Holocene sea level changes in the Netherlands. *Mededelingen Geologische Stichting* **7**: 1–100.

Jelgersma S. 1966. Sea-level changes during the last 10,000 years. In *Proceedings of the International Symposium on World Climate from 8000 to 0 B.C.* London: Royal Meteorological Society; 54–71.

Katsman CA, Sterl A, Beersma JJ *et al.* 2011. Exploring high-end scenarios for local sea level rise to develop flood protection strategies for a low-lying delta—the Netherlands as an example. *Climatic Change* **109**: 617–645.

Kiden P. 1995. Holocene relative sea-level change and crustal movement in the southwestern Netherlands. *Marine Geology* **124**: 21–41.

Kiden P, Denys L, Johnston P. 2002. Late Quaternary sea-level change and isostatic and tectonic land movements along the Belgian-Dutch North Sea coast: geological data and model results. *Journal of Quaternary Science* **17**: 535–546.

Kiden P, Makaske B, Van de Plassche O. 2008. Waarom verschillen de zeespiegelreconstructies voor Nederland? *Grondboor en Hamer* **3/4**: 54–61.

Kiden P, Vos PC. 2012. Holocene relative sea-level change and land movements in the northern Netherlands – a first assessment. In *3rd IGCP588-Conference 'Preparing for Coastal Change' Conference Program* - Book of Abstracts. Christian-Albrechts-Universität Zu Kiel, Germany; 22.

KNMI. 2014. KNMI'14: climate Change scenarios for the 21st Century – A Netherlands perspective. *Scientific Reports* WR2014-01. www.climatescenarios.nl. De Bilt: KNMI.

Kopp RE, Horton RM, Little CM *et al.* 2014. Probabilistic 21st and 22nd century sea-level projections at a global network of tide-gauge sites. *Earth's Future* **2**: 383–406.

Kopp RE, Kemp AC, Bittermann KBP *et al.* 2016. Temperature-driven global sea-level variability in the Common Era. *Proceedings of the National Academy of Sciences of the United States of America* **113**: E1434–E1441.

Lambeck K, Smither C, Johnston P. 1998. Sea-level change, glacial rebound and mantle viscosity for northern Europe. *Geophysical Journal International* **134**: 102–144.

Lowe JA, Howard TP, Pardaens A *et al.* 2009. *UK Climate Projections science report: marine and coastal projections*. Exeter: Met Office, Hadley Centre.

Ludwig G, Müller H, Streif H. 1981. New dates on Holocene sea-level changes in the German Bight. In *Holocene Marine Sedimentation in the North Sea Basin*, Nio SD, Shüttenhelm RTE, Van Weering TjCE (eds). London: Blackwell Publishing.

McHutchon A, Rasmussen CE. 2011. Gaussian process training with input noise. *Advances in Neural Information Processing Systems* **24**: 1341–1349.

Mook WG. 2005. Introduction to isotope hydrology. *IAH Series International Contributions to Hydrogeology*. London: Taylor & Francis.

Mook WG, Streurman HJ. 1983. *Physical and Chemical Aspects of Radiocarbon Dating*. PACT Publications 8; 31–55.

Mook WG, Van de Plassche O. 1986. Radiocarbon dating. In *Sea Level Research, a Manual for the Collection and Evaluation of Data*, Van de Plassche O (ed.). Norwich: Geobooks; 525–560.

Morton RA, White WA. 1997. Characteristics of and corrections for core shortening in unconsolidated sediments. *Journal of Coastal Research* **13**: 761–769.

Nieuwhof A, Vos PC. 2018. New data from terp excavations on sea-level index points and salt marsh sedimentation rates in the eastern part of the Dutch Wadden Sea. *Netherlands Journal of Geosciences* **97**: 31–43.

Oost AP. 1995. *Dynamics and sedimentary developments of the Dutch Wadden Sea with a special emphasis on the Frisian Inlet: a study of the barrier islands, ebb-tidal deltas, inlets and drainage basins*. PhD Dissertation. Utrecht University.

Oost AP, Hoekstra P, Wiersma A *et al.* 2012. Barrier island management: lessons from the past and directions for the future. *Ocean & Coastal Management* **68**: 18–38.

Rasmussen CE, Williams CKI. 2006. *Gaussian Processes for Machine Learning*. Cambridge: MIT Press.

Simpson M, Ravndal O, Sande H *et al.* 2017. Projected 21st century sea-level changes, observed sea level extremes, and sea level allowances for Norway. *Journal of Marine Science and Engineering* **5**: 36.

Reimer PJ, Bard E, Bayliss A, van der Plicht J *et al.* 2013. IntCal13 and Marine13 Radiocarbon age calibration curves 0–50,000 years cal BP. *Radiocarbon* **55**: 1869–1887.

Rijkswaterstaat. 2011. Kenmerkende waarden getijgebied 2011. https://staticresources.rijkswaterstaat.nl/binaries/Kenmerkende%20waarden%20getijgebied%202011_tcm21-97249.pdf. Last accessed: 11 January 2018.

Roeleveld W. 1974. *The Holocene evolution of the Groningen marine-clay district*. PhD Thesis, Free University of Amsterdam.

Roep TB, Beets DJ. 1988. Sea level rise and palaeotidal levels from sedimentary structures in the coastal barriers in the western Netherlands since 5600 BP. *Geologie en Mijnbouw* **67**: 53–61.

Röper T, Kröger KF, Meyer H *et al.* 2012. Groundwater ages, recharge conditions and hydrochemical evolution of a barrier island freshwater lens (Spiekeroog, Northern Germany). *Journal of Hydrology* **454–455**: 173–186.

Shennan I. 1986. Flandrian sea-level changes in the Fenland. II: Tendencies of sea-level movement, altitudinal changes, and local and regional factors. *Journal of Quaternary Science* **1**: 155–179.

Shennan I, Bradley S, Milne G *et al.* 2006. Relative sea-level changes, glacial isostatic modelling and ice-sheet reconstructions from the British Isles since the last glacial maximum. *Journal of Quaternary Science* **21**: 585–599.

Shennan I, Horton BP. 2002. Holocene land- and sea-level changes in Great Britain. *Journal of Quaternary Science* **17**: 511–526.

Shennan I, Lambeck K, Flather R *et al.* 2000. Modelling western North Sea palaeogeographies and tidal changes during the Holocene. In *Holocene Land-Ocean Interaction and Environmental Change Around the North Sea, Special Publications 166*, Shennan I, Andrews J (eds). London: Geological Society; 299–319.

Shennan I, Milne GA, Bradley S. 2012. Late Holocene vertical land motion and relative sea-level changes: lessons from the British Isles. *Journal of Quaternary Science* **27**: 64–70.

Smith DE, Harrison S, Firth CR *et al.* 2011. The early Holocene sea level rise. *Quaternary Science Reviews* **30**: 1846–1860.

Speelman H, Oost A, Verweij H *et al.* 2009. De ontwikkeling van het Waddengebied in tijd en ruimte. Position paper geosciences. Leeuwarden: Waddenacademie.

Streif H. 1989. Barrier islands, tidal flats, and coastal marshes resulting from a relative rise of sea level in East Frisia on the German North Sea coast. In *Proceedings KNGMG symposium 'Coastal Lowlands, Geology and Geotechnology'*. Dordrecht: Kluwer Academic Publishers; 213–223.

Streif H. 2004. Sedimentary record of Pleistocene and Holocene marine inundations along the North Sea coast of Lower Saxony, Germany. *Quaternary International* **112**: 3–28.

Törnqvist TE, De Jong AFM, Oosterbaan WA *et al.* 1992. Accurate dating of organic deposits by AMS ^{14}C measurement of macrofossils. *Radiocarbon* **34**: 566–577.

Törnqvist TE, González JL, Newsom LA *et al.* 2004. Deciphering Holocene sea-level history on the U.S. Gulf Coast: A high-resolution record from the Mississippi Delta. *Geological Society of America Bulletin* **116**: 1026–1039.

Törnqvist TE, Van Ree MHM, van 't Veer R *et al.* 1998. Improving methodology for high-resolution reconstruction of sea-level rise and neotectonics by paleoecological analysis and AMS ^{14}C dating of basal peats. *Quaternary Research* **49**: 72–85.

Tronicke J, Blindow N, Groß R *et al.* 1999. Joint application of surface electrical resistivity- and GPR-measurements for groundwater exploration on the island of Spiekeroog – northern Germany. *Journal of Hydrology* **223**: 44–53.

Uehara K, Scourse JD, Horsburgh KJ *et al.* 2006. Tidal evolution of the northwest European shelf seas from the Last Glacial Maximum to the present. *Journal of Geophysical Research* **111**: C09025.

UNESCO. 2009. whc.unesco.org/en/list/1314. Last accessed: 14 December 2017.

Van de Meene EA, Van der Staay J, Hock TL 1979. The van der Staay suction-corer – A simple apparatus for drilling in sand below groundwater table. *Rijks Geologische Dienst* **15-1-1979**: 1–26.

Van de Plassche O. 1980. Holocene water-level changes in the Rhine-Meuse Delta as a function of changes in relative sea level, local tidal range, and river gradient. *Geologie en Mijnbouw* **59**: 343–351.

Van de Plassche O. 1981. Sea level, groundwater, and basal peat growth – a reassessment of data from the Netherlands. *Geologie en Mijnbouw* **60**: 401–408.

Van de Plassche O. 1982. Sea-level change and water-level movements in the Netherlands during the Holocene. *Mededelingen Rijks Geologische Dienst* **36**: 1–93.

Van de Plassche O, Bohncke SJP, Makaske B, van der Plicht J *et al.* 2005. Water-level changes in the Flevo area, central Netherlands (5300–1500 BC): implications for relative mean sea-level rise in the Western Netherlands. *Quaternary International* **133–**134: 77–93.

Van de Plassche O, Makaske B, Hoek WZ, van der Plicht J *et al.* 2010. Mid-Holocene water-level changes in the lower Rhine-Meuse Delta (western Netherlands): implications for the reconstruction of relative mean sea-level rise, palaeoriver-gradients and coastal evolution. *Netherlands Journal of Geosciences* **89**: 3–20.

Van de Plassche O, Roep TB. 1989. Sea-level changes in the Netherlands during the last 6500 years: basal peat vs. coastal barrier data. In *Late Quaternary Sea-Level Correlation and Application*, Scott DB, Pirazolli PA, Honig CA (eds). NATO ASI Ser. C256. Dordrecht: Kluwer Publishers: 41–56.

Van der Molen J, de Swart HE. 2001. Holocene tidal conditions and tide-induced sand transport in the southern North Sea. *Journal of Geophysical Research: Oceans* **106**: 9339–9362.

Van der Plicht J, Wijma S, Aerts AT *et al.* 2000. The Groningen AMS facility: status report. *Nuclear Instruments and Methods* **B172**: 58–65.

Van der Spek AJF. 1996. Holocene depositional sequences in the Dutch Wadden Sea south of the island of Ameland. *Mededelingen Rijks Geologische Dienst* **57**: 41–68.

Van der Spek AJF. 1994. *Large-scale evolution of Holocene tidal basins in the Netherlands*. – PhD Thesis, University Utrecht.

Van der Zon N. 2013. *Kwaliteitsdocument AHN2*. Delft: Rijkswaterstaat.

Van Staalduinen CJ. 1977. *Geologisch onderzoek van het Nederlandse Waddengebied*. Haarlem: Rijks Geologische Dienst.

Van Straaten LMJU. 1954. Radiocarbon datings and changes of sea level at Velzen (Netherlands). *Geologie en Mijnbouw* **16**: 247–253.

Vermeersen LLA, Slangen ABA, Gerkema T, *et al.* accepted. Sea-level change in the Dutch Wadden Sea. *Netherlands Journal of Geosciences* **97**(3): xx–xx. https://doi.org/10.1017/njg.2018.7

Vink A, Steffen H, Reinhardt L *et al.* 2007. Holocene relative sea-level change, isostatic subsidence and the radial viscosity structure of the mantle of northwest Europe (Belgium, the Netherlands, Germany, southern North Sea). *Quaternary Science Reviews* **26**: 3249–3275.

Vogel JC, Waterbolk HT. 1963. Groningen Radiocarbon dates IV. *Radiocarbon* **5**: 163–202.

Vos P. 2015. *Origin of the Dutch coastal landscape. Long-term landscape evolution of the Netherlands during the Holocene, described and visualized in national, regional and local palaeogeographical map series*. PhD dissertation, Deltares.

Vos PC. 2006. *Toelichting bij de nieuwe paleogeografische kaarten van Nederland. Nationale Onderzoeksagenda Archeologie (NOaA)*. Amersfoort: Rijksdienst voor het Cultureel Erfgoed.

Vos PC, De Vries S. 2015. 2nd generation palaeogeographical maps from the Netherlands (version 2.0). Deltares, Utrecht. Retrieved from: www.archeologieinnederland.nl.

Vött A. 2007. Relative sea level changes and regional tectonic evolution of seven coastal areas in NW Greece since the mid-Holocene. *Quaternary Science Reviews* **26**: 894–919.

Whitehouse PL. 2018. Glacial isostatic adjustment modelling: historical perspectives, recent advances, and future directions. *Earth Surface Dynamics* **6**: 401–429.

Woldring H, De Boer P, Bottema-Mac Gillavry JN *et al.* 2005. De palaeoecology van Duurswold (Gr.): vroeg-Holocene landschapsontwikkeling. *Paleo-Aktueel* **17**: 36–44.

